ARTHROPOD SYSTEMATICS & PHYLOGENY

75 (3): 387–415
20.12.2017

SENCKENBERG

A revision of the wolf spider genus *Diapontia* Keyserling, and the relationships of the subfamily Sosippinae (Araneae: Lycosidae)

Luis Norberto Piacentini *[1], Cristina Luisa Scioscia[1], Mirta Noemí Carbajal[2], Ricardo Ott[3], Antonio Domingo Brescovit[4] & Martín Javier Ramírez[1]

[1] División Aracnología, Museo Argentino de Ciencias Naturales "Bernardino Rivadavia" – CONICET, Av. Angel Gallardo 470, C1405DJR Buenos Aires, Argentina; Luis Norberto Piacentini [piacentini@macn.gov.ar]; Cristina Luisa Scioscia [scioscia@macn.gov.ar]; Martín Javier Ramírez [ramirez@macn.gov.ar] — [2] Fundación Inalafquen. H. Yrigoyen 792. 8520 San Antonio Oeste, Río Negro, Argentina; Mirta Noemí Carbajal [diapontia@gmail.com] — [3] Museu de Ciências Naturais, Fundação Zoobotânica do Rio Grande do Sul, Rua Dr. Salvador França, 1427, 90690-000 Porto Alegre, RS, Brazil; Ricardo Ott [rott@fzb.rs.gov.br] — [4] Laboratório Especial de Coleções Zoológicas, Instituto Butantan, Av. Vital Brasil, 1500, Butantã, São Paulo, São Paulo, Brazil, CEP 05503-900; Antonio Brescovit [adbresc@terra.com.br] — *Corresponding author

Accepted 21.vi.2017.
Published online at www.senckenberg.de/arthropod-systematics on 11.xii.2017.

Editors in charge: Lorenzo Prendini & Klaus-Dieter Klass

Abstract

The South American genus *Diapontia* is revised to include nine species: *Diapontia uruguayensis* Keyserling, 1877 (= *Diapontia senescens* Mello-Leitão, 1944 **syn.n.**; *D. infausta* Mello-Leitão, 1941 **syn.n.**; *D. pourtaleensis* Mello-Leitão, 1944 **syn.n.**; *D. albopunctata* Mello-Leitão, 1941 **syn.n.**) from northern Paraguay, southeastern Brazil, southern Uruguay, southern to northeastern Argentina and southern Chile; *D. niveovittata* Mello-Leitão, 1945 from southern Paraguay, north-central Argentina and southern Brazil; *D. anfibia* (Zapfe-Mann, 1979) **comb.n.** (= *Lycosa artigasi* Casanueva, 1980 **syn.n.**) from central and southern Chile and southwestern Argentina, transferred from *Pardosa* C.L. Koch, 1847; *D. securifera* (Tullgren, 1905) **comb.n.** from northern Chile and northwestern Argentina, transferred from *Orinocosa* Chamberlin, 1916; *D. arapensis* (Strand, 1908) **comb.n.**, from Peru, transferred from *Hippasella* Mello-Leitão, 1944; *D. calama* **sp.n.** from northern Chile; *D. songotal* **sp.n.** from southern Bolivia; *D. chamberlini* **sp.n.** from central and southern Peru; and *D. oxapampa* **sp.n.** from northern Peru. The sister-group relationship between *Diapontia* and *Hippasella*, and their placement in the subfamily Sosippinae, were supported by phylogenetic analyses based on four molecular markers (28S, 12S, NADH1 and COI), using Bayesian inference and maximum-likelihood. We tested whether DNA barcoding techniques were able to corroborate the identity of four *Diapontia* species. *Diapontia securifera* and *D. anfibia* were successfully identified using COI; however, *D. niveovittata* and *D. uruguayensis* were found to share identical haplotypes and thus could not be discriminated.

Key words

Lycosids, DNA barcoding, systematics, new species, South America, Andean, Neotropical, Bayesian analysis, natural history.

1. Introduction

New exciting developments in spider phylogenetics (Ramírez 2014; Polotow et al. 2015; Wheeler et al. 2017) have brought many neglected groups into the bigger picture of spider evolution. In this contribution, we specifically trace the evolutionary history of one peculiar genus, *Diapontia* Keyserling, 1877, that belongs to the family Lycosidae Sundevall, 1833, which is commonly known as the wolf spiders. This family represents a relatively

recent radiation of arachnids (Jocqué & Alderweireldt 2005; Garrison et al. 2016) and has a worldwide distribution. The Lycosidae are clearly delimited from other families based on somatic, behavioural and molecular characters (Dondale 1986; Wheeler et al. 2017) and exhibit a wide range of prey-capture strategies including burrow-dwelling, vagrant, and web building species (Dondale & Redner 1990). In the Americas, two web building genera have been reported: *Sosippus* Simon, 1888 from North and Central America (see Brady 2007), and *Aglaoctenus* Tullgren, 1905 from South America (see Santos & Brescovit 2001; Santos et al. 2003; Piacentini 2011). Dondale (1986) recognized the close relationship between *Sosippus* and *Aglaoctenus* and erected the subfamily Sosippinae for these two genera, placing them as the sister-group to all other lycosids. Although the subfamily was recovered as monophyletic in a molecular analysis using two markers (12S and NADH1), the relationships among subfamilies remained uncertain and had little support (Murphy et al. 2006: figs. 2, 3). The 28S marker was excluded of the analysis performed by Murphy et al. (2006: fig. 6) who suspected that there were paralogous copies of 28S due to the implausible trees it produced.

Three characters of the male bulb were proposed by Dondale (1986) as diagnostic for Sosippinae: the loss of the terminal apophysis, a tegular groove functioning as a conductor, and the embolus lying among a cluster of tegular processes. However, Sierwald (2000) later questioned those characters pointing out that the loss of the terminal apophysis can be a plesiomorphy and the conductor function cannot be evaluated since the function of various parts of the palp is unclear. In a redescription of *Aglaoctenus oblongus* (C.L. Koch, 1847), the curved apophysis at the base of the embolus (labeled as "apophysis b" by Sierwald 2000) was proposed as an additional diagnostic character (Santos et al. 2003). The composition of the subfamily was later modified by Álvares & Brescovit (2007) who redescribed *Hippasella guaquiensis* (Strand, 1908), the type species of the genus *Hippasella* Mello-Leitão, 1944 and placed it in Sosippinae; they also suggested that *Diapontia* should be placed in the same subfamily.

Keyserling (1877) described the genus *Diapontia* to accommodate three new species of South American lycosids, but he did not designate a type species. The genus was considered a junior synonym of *Lycosa* by Simon (1898). However, Petrunkevitch (1911) rejected the synonymy, revalidated the genus, and established *Diapontia uruguayensis* Keyserling, 1877 as the type species.

Lycosid species are often distinguished by small differences in the genitalia which presents a challenge to the identification of species, particularly for non-taxonomists. Recent studies have begun to use DNA barcoding as a tool to help identify species of wolf spiders (Blagoev et al. 2013; Sim et al. 2014; Blagoev & Dondale 2014; Astrin et al. 2016; Nadonly et al. 2016). Although barcoding methods seem to work well in general, each of these studies identified groups of closely related species that exhibited low genetic distances and subtle morphological differences, suggesting a recent divergence. This agrees with the ideas proposed by Jocqué & Alderweireldt (2005), namely that Lycosidae is a family with a recent origin, based on characteristics of the morphology, habitat preference and the scarce fossil record. In a phylogenomic analysis, age estimates suggest that Lycosidae are among among the most recently derived families of spiders, having separated from pisaurids about 37 million years ago (Garrison et al. 2016); however, because Trechaleidae, the sister family of Lycosidae (Wheeler et al. 2017; Albo et al. 2017), was not included in the analysis, an estimated age for the origin of lycosids is not available.

The aim of this study is to review the genus *Diapontia* and describe four new species, test the subfamiliar placement of the genus and the relationships of Sosippinae among wolf spiders, and evaluate DNA barcoding as a method for species identification within this genus.

2. Material and methods

2.1. Figures

Drawings were made using a camera lucida mounted on an Olympus BH−2 compound microscope or a Leica M165 C stereoscopic microscope. The internal genitalia were cleared in clove oil and, in the case of non-type specimens, digested with Enzymatic Cleaner (Ultrazyme®). When several males were available for study, the male bulb was removed to clarify the morphology of its sclerites. Photographs of preserved specimens were taken with a Leica DFC 290 digital camera mounted on a Leica M165 C stereoscopic microscope. Images taken in different focal planes were combined with Helicon Focus 4.62 Pro (www.heliconsoft.com). Measurements are given in millimetres. Distribution maps were compiled with Simple Mappr (http://www.simplemappr.net). Geographic coordinates of localities were estimated in Google Earth (www.google.com/earth) if not otherwise provided.

2.2. Abbreviations

Morphology: **A**, atrium; **Ac**, aciniform gland spigot; **AER**, anterior eye row; **AL**, abdomen length; **ALE**, anterior lateral eye; **ALS**, anterior lateral spinneret; **AME**, anterior median eye; **BS**, base of the spermatheca; **C**, conductor; **c**, ventral projection of tegulum; **CH**, carapace height; **CL**, carapace length; **CP**, copulatory plug; **Cy**, cylindrical gland spigot; **CW**, carapace width, taken in the fovea zone; **E**, embolus; **FD**, fertilization duct; **HS**, head of spermatheca; **LAC**, lateral apophysis of conductor; **MA**, median apophysis; **PLE**, posterior lateral eye; **PLER**, posterior lateral eye row; **PLS**, posterior lateral spinneret; **PME**, posterior median eye; **PMER**, posterior median eye row; **PMS**, posterior median spinneret; **MAP**,

Table 1. List of GenBank or BOLDSYSTEM reference numbers of terminals used in the Bayesian analysis.

Family	Species	28S	12S	NADH	COI
Lycosidae	*Allocosa senex*	MF410705	MF410703	MF410712	SPDAR375-14
Lycosidae	*Gnatholycosa spinipalpis*	MF410707	—	MF410714	SPDAR973-15
Lycosidae	*Anoteropsis adumbrata*	DQ019749	DQ019762	DQ019650	AY059962
Lycosidae	*Artoria separata*	DQ019748	DQ019772	DQ019659	AY059993
Lycosidae	*Xerolycosa nemoralis*	MF410710	DQ019821	DQ019710	NOARA114-11
Lycosidae	*Geolycosa missouriensis*	DQ019727	DQ019775	DQ019662	—
Lycosidae	*Lycosa erythrognatha*	DQ019729	DQ019782	DQ019670	SPDAR371-14
Lycosidae	*Pardosa astrigera*	JN816974	DQ019792	DQ019685	AY836013
Lycosidae	*Pardosa californica*	DQ019719	DQ019794	DQ019687	—
Lycosidae	*Pirata subpiraticus*	JN816979	DQ019804	DQ019698	JN817187
Lycosidae	*Piratula hygrophila*	MF410708	DQ019801	DQ019696	NLARA214-12
Lycosidae	*Aglaoctenus lagotis*	—	DQ019753	DQ019640	ACI9466
Lycosidae	*Diapontia uruguayensis*	MF410706	MF410704	MF410713	ACY4931
Lycosidae	*Hippasella alhue*	MF461286	—	MF410715	SPDAR956-15
Lycosidae	*Sosippus placidus*	DQ019752	DQ019808	DQ019702	DQ151823
Lycosidae	*Anomalosa kochi*	DQ019722	DQ019761	DQ019649	—
Lycosidae	*Venonia micaroides*	DQ019738	DQ019819	DQ019709	—
Lycosidae	*Zoica* sp.	MF410711	—	MF410717	—
Pisauridae	*Dolomedes* sp.	DQ019726	DQ019774	DQ019661	KX537485
Pisauridae	*Thaumasia velox*	MF410709	—	MF410718	SPDAR967-15
Trechaleidae	*Paratrechalea ornata*	KY190293	—	MF410716	—
Trechaleidae	*Trechaleoides biocellata*	KY017475	KY015653	—	SPDAR403-14
Thomisidae	*Tmarus* sp.	KM225076	—	—	SPDAR844-14
Oxyopidae	*Oxyopes* sp.	KM225064	KY016011	—	SPDAR550-14

mayor ampullate gland spigot; **mAP**, minor ampullate gland spigot; **S**, septum; **SS**, stalk of spermatheca; **TL**, total length; **VC**, vulval chamber.

Collections: **AMNH**, American Museum of Natural History, New York, USA; **CASENT**, California Academy of Sciences, California, USA; **FCE**, Facultad de Ciencias, Montevideo, Uruguay; **IBSP**, Instituto Butantan, São Paulo, Brazil; **MACN-Ar**, Museo Argentino de Ciencias Naturales "Bernardino Rivadavia", Buenos Aires, Argentina; **MCN**, Museu de Ciências Naturais da Fundação Zoobotânica do Rio Grande do Sul, Porto Alegre, Brazil; **MCZ**, Museum of Comparative Zoology, Massachusetts, USA; **MLP**, Museo de La Plata, Argentina; **MNHN**, Museo Nacional de Historia Natural, Santiago, Chile; **MUSM**, Museo de Historia Natural, Lima, Peru; **MZUC-UCCC**, Museo de Zoología de la Universidad de Concepción, Chile; **NHAM**, Naturhistoriska Riksmuseet, Stockholm, Sweden; **BMNH**, Natural History Museum, London, England; **USNM**, National Museum of Natural History, Washington, USA.

2.3. Terminology

Species descriptions and measurements follow Piacentini & Grismado (2009). The notation for macrosetae follows Ramírez (2003). The nomenclature of the genital elements follows Sierwald (2000), Langlands & Framenau (2010) and Logunov (2010). Details of the non-type specimens that were examined are listed in Electronic Supplement File 1 with a summary of localities provided in the Distribution section for each species.

Table 2. Primers used for the amplification and sequencing of DNA in this study.

Locus	Primer	Reference	Size of fragment
28S	28S "O"	Hedin & Maddison 2001	800 bp
	28S "C"		
12S	12S-ai	Kocher et al. 1989	335 bp
	12S-bi		
NADH1	TL-1-N-12718	Hedin 1997	600 bp
	M510	Murphy et al. 2006	

2.4. Molecular data

Sequence data from previous work on lycosids (Murphy et al. 2006; Polotow et al. 2015; Wheeler et al. 2017) were accessed via GenBank and new sequence data were generated in the molecular lab at the MACN. Nine of the eleven currently recognized lycosid subfamilies, as well as exemplars of the Pisauridae, Trechaleidae, Thomisidae and Oxyopidae, were represented in the dataset (see Table 1 for accession numbers and specimen details). The sequences of COI used in the DNA barcoding analyses were from specimens submitted by us to the Barcode of Life Data System (BOLD; Ratnasinham & Hebert 2007) (see Table S2.4 in Electronic Supplement File 2 for accession numbers and specimen details). Genomic DNA was extracted from muscle tissue taken from the leg of each specimen using the Qiagen DNeasy Blood and Tissue Kit or with the Chelex extraction following the protocol proposed by Casquet et al. (2012) modified by an additional final step of heating the samples for 20 min at 100ºC.

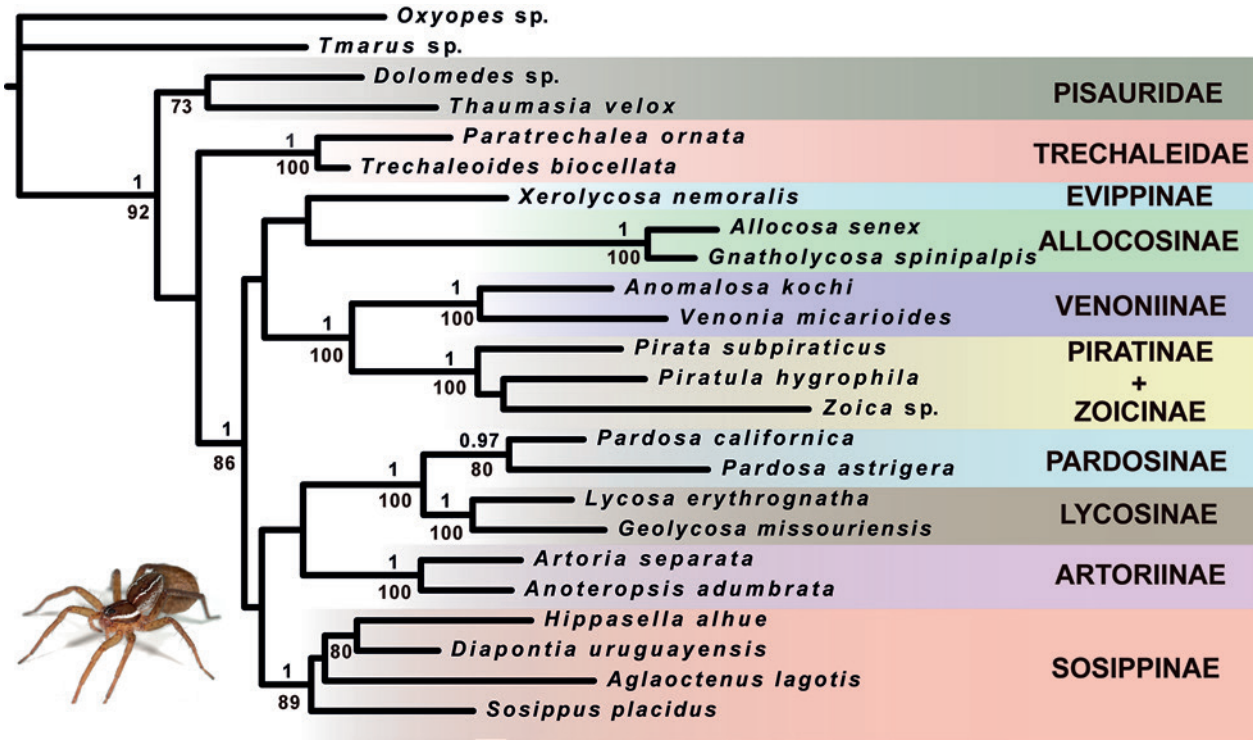

Fig. 1. Bayesian inference tree of Lycosidae and outgroup taxa, based on a combined analysis of 28S, 12S, NADH and COI gene fragments (2,132 base pairs). Values above branches are posterior probabilities, below branches are ML bootstrap values (support values below 0.95 and 50, respectively, are not shown).

Four gene loci were selected to test the subfamily placement of *Diapontia* because they evolve at different rates and provide phylogenetic resolution at different, overlapping taxonomic levels. Primers for each locus are given in Table 2. The barcode region of the cytochrome c oxidase subunit I (COI) gene obtained from BOLD was 658 bp. Details of PCR conditions, such as reagent mix composition and thermal profiles follows Murphy et al. (2006) except for 28S, for which a double cycle was performed with an initial step of 95°C for 5 min, followed by 10 cycles of 95°C for 30 s, an annealing temperature of 56°C for 30 s and an extension temperature of 72°C for 45 s, then 25 cycles with an anneling temperature of 54°C.

Bioedit v. 7.2.5 (Hall 1999) was used to view chromatograms and edit raw sequence data for the four gene loci. Alignments of protein-encoding genes (COI and NADH1) were trivial due to the lack of gaps. To align the ribosomal genes, we used the online version of MAFFT v.7 (Katoh & Standley 2013), by applying the "Auto" strategy and a gap-opening penalty of 1.53 and the output alignment was processed with the online version of GBlocks (Castresana 2000) to remove positions of ambiguous homology. Nucleotide composition homogeneity tests were conducted separately on the alignments of each locus (and codon position for COI and NADH1) using Tree-Puzzle v. 5.2 (Schmidt et al. 2002) to verify, based on a chi-squared test, whether all partitions were appropriate for phylogenetic reconstruction (Rosenberg & Kumar 2003). The program Partitionfinder v 1.1.1 (Lanfear et al. 2012) was used to select the best partition schema and the fitting model of evolution for each partition using the Akaike's information criterion. Bayesian analysis was performed using MrBayes 3.2.6 (Ronquist et al. 2012) through on the CIPRES Science Gateway (Miller et al. 2010). The tree search was conducted with two independent analyses consisting of one cold and three heated MCMC chains with 20.000.000 generations and sampling every 2000 generations (ngen=20.000.000 printfreq=2.000 samplefreq=2000 nruns=2 nchains=4). The first 25% of each search was discarded as 'burn-in' (burninfrac=0.25). The program TRACER ver. 1.6 (Rambaut et al. 2014) was used to ensure that the Markov chains had reached stationarity by examining the effective sample size values (above 200). Maximum likelihood analysis was performed with RAxML version 8.2.9 (Stamatakis 2014) through the CIPRES Science Gateway (Miller et al. 2010) with default settings. For the DNA barcoding analysis, we used the tools provided by the Barcode of Life Data System (BOLD; Ratnasingham & Hebert 2007) to perform the nearest neighbour analyses as in Nadolny et al. (2016).

3. Results

3.1. Subfamily placement

The molecular markers 28S, 12S and COI passed the homogeneity test and therefore did not require any transformation. However, the third codon position of NADH1

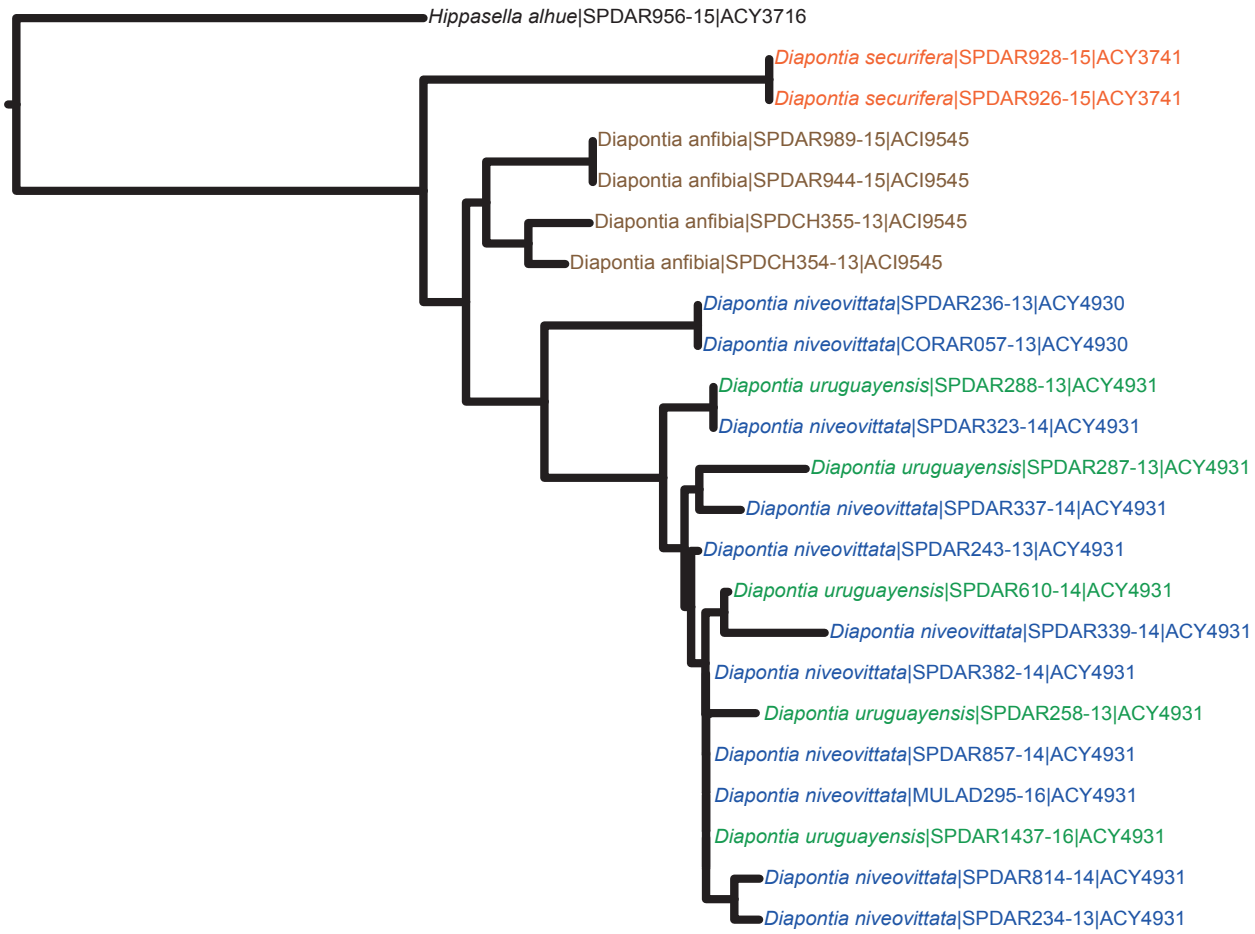

Fig. 2. Neighbour-joining tree obtained of the analysis of COI gene fragment through of BOLDSYSTEM platform showing the relationships for species of *Diapontia* Keyserling. Data presented as: Species name | BOLD Process ID | BIN number. Each color represents a different species.

failed the test for homogeneity and therefore we substituted R for adenine and guanine and Y for cytosine and thymine after which it passed the homogeneity test. Results of the PartitionFinder analysis indicated that the best partition scheme for COI was to model each codon position independently. Thus, we ran six partitions: 28S, 12S, NADH1, COI_1, COI_2 and COI_3. For 28S, 12S and NADH1 the best-fit model GTR+G was applied. The best fit model TVM+I+G was selected for COI_1 and COI_3, and F81+I for COI_2.

Murphy et al. (2006) questioned the utility of 28S in their lycosid phylogeny due to the presence of paralogous copies in some of their terminals; however, for the taxa selected in this study, the 28S gene tree topology agreed with those obtained using the mithochondrial markers, thus we used the marker in our analyses.

The final matrix was composed of 24 taxa and 2132 characters (583 from 28S, 279 from 12S, 613 from NADH1, and 657 from COI). The resulting tree had high posterior support for the monophyly of families and subfamilies (Fig. 1) and supports the placement of *Diapontia* in Sosippinae. The tree obtained in the maximum likelihood analysis (Fig. S2.5 in Electronic Supplement File 2) has a topology similar to that of the Bayesian tree, except for the relative position of three groups with low support: *Xerolycosa* as sister group of Venoniinae + Piratinae + Zoicinae instead of sister of Allocosinae; Allocosinae as sister group of Lycosinae + Pardosinae instead of *Xerolycosa*; and *Aglaoctenus*, which emerged in a clade with *Sosippus* instead of sister to *Hippasella* + *Diapontia*. High boostrap values were obtained for families and subfamilies, which are summarized in the Bayesian tree (Fig. 1).

3.2. DNA barcode analysis

For the DNA barcode analysis, we obtained twenty sequences from four *Diapontia* species, with a length of 658 bp (except MACN-Ar 31393, with 624 bp). The four species for which barcode data were examined were separated on four BINs (Ratnasingham & Hebert 2013) (Fig. 2): ACI9545, composed of specimens of *D. anfibia*; ACY3741, composed of specimens of *D. securifera*; ACY4930, composed of two specimens of *D. niveovittata*; and ACY4931, composed of specimens of *D. uruguayensis* and *D. niveovittata*.

The mean intraspecific divergence (MID) and the maximum intraspecific divergence (MXID) are summarized in Table S2.2 in Electronic Supplement File 2. *Dia-*

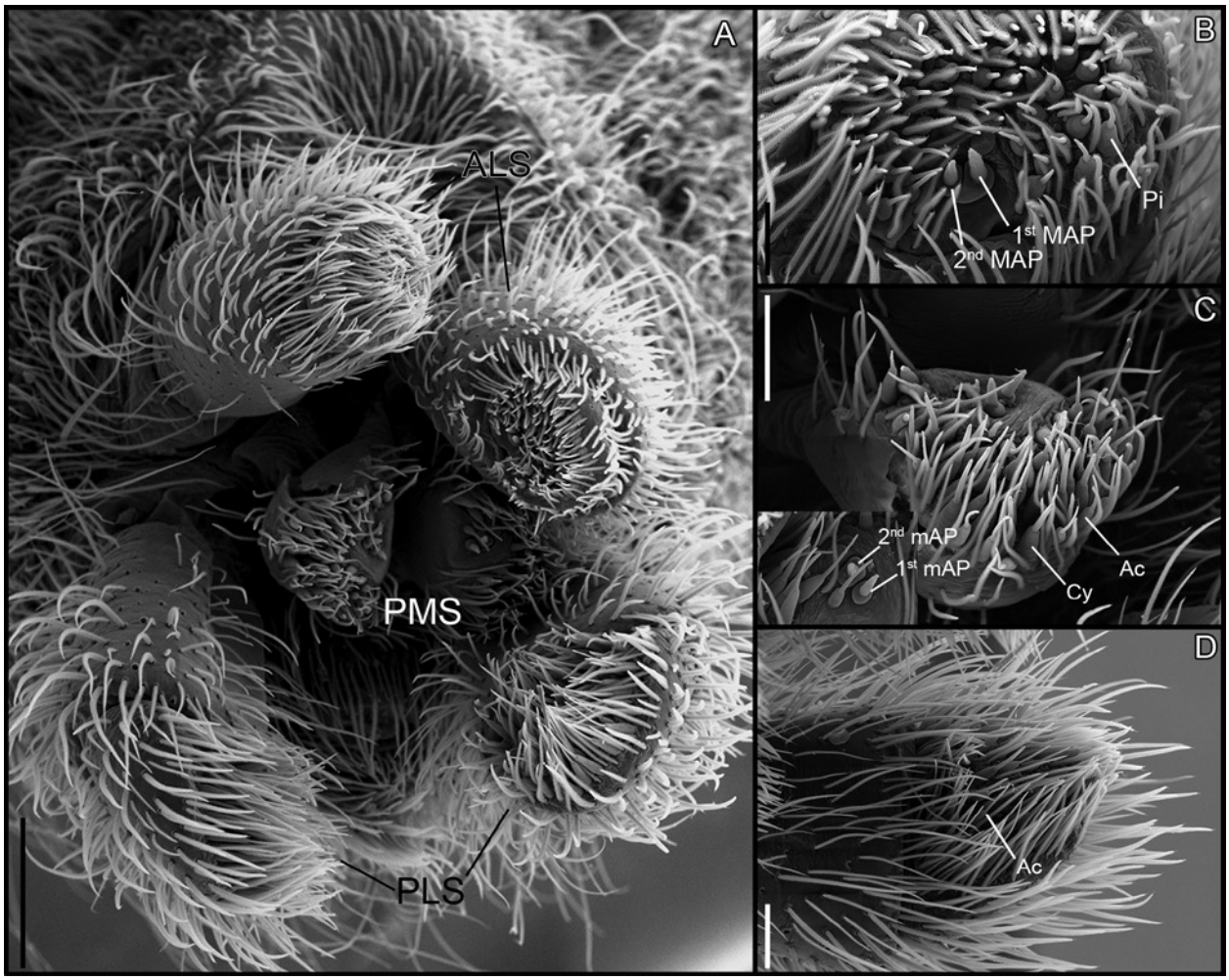

Fig. 3. *Diapontia niveovittata* Mello-Leitão female. **A**: Spinnerets posteroventral view. **B**: ALS spinning field. **C**: PMS spinning field, bottom left, mAP field detail. **D**: PLS spinning field — ***Abbreviations***: Ac, aciniform spigot; ALS, anterior lateral spinnerets; Cy, cylindrical spigot; mAP, minor ampullate gland; MAP, mayor ampullate gland; Pi, piriform gland spigots; PLS, posterior lateral spinnerets; PMS, posterior median spinnerets. — ***Scale bars***: A 0.50 mm; B 0.10 mm; C,D 0.20 mm.

pontia anfibia is recovered in two groups, one composed of specimens from the Argentinian provinces of Chubut and Río Negro, with identical sequences and the other of two specimens of Bío Bío, Chile, and these groups are separated by 1.23% of divergence. The specimens of *Diapontia uruguayensis* emerged in a clade that also contains representatives of *D. niveovittata*, and the mean divergence of the group is 1.12% with a maximum divergence of 2.49%. The minimal divergence observed between the *D. niveovittata* and *D. uruguayensis* was zero since there were specimens with identical sequences. As founded on other lycosids (Correa-Ramírez et al. 2010), most of the differences on the sequences are silent mutations, except for three on *D. securifera* specimens and the other in one specimen of *D. niveovittata* (MACN-Ar 31348).

Results of the nearest neighbour analysis (Fig. S2.3 in Electronic Supplement File 2) showed the presence of DNA barcoding gap between *D. securifera* and *D. anfibia*, and its absence between *D. uruguayensis* and *D. niveovittata*, as expected due to the existence of identical sequences for those species (Hebert et al. 2003; Meyer & Paulay 2005).

3.3. Taxonomy

Lycosidae Sundevall, 1833
Sosippinae Dondale, 1986

3.3.1. Genus *Diapontia* Keyserling, 1877

Diapontia Keyserling, 1877: 675 (type species *D. uruguayensis* Keyserling, subsequent designation by Petrunkevitch 1911: 553). Roewer 1955: 240. Roewer 1960: 756. Petrunkevitch 1911: 553 (Reval.).
Lycosa: Simon, 1898: 347 (Syn.).

Differential diagnosis. The absence of terminal apophysis and the presence of a lateral apophysis on the conductor identify *Diapontia* as a member of the lycosid subfamily Sosippinae. Within this subfamily, males can be distinguished from the remaining Sosippinae by the S-shaped trajectory of the sperm duct (Fig. 7C) and females by the short stalk of the spermatheca (Fig. 7G).

Description. Medium-sized wolf spiders. Total length 6.52–18.36; carapace length 2.93–7.71, width 2.00–5.60,

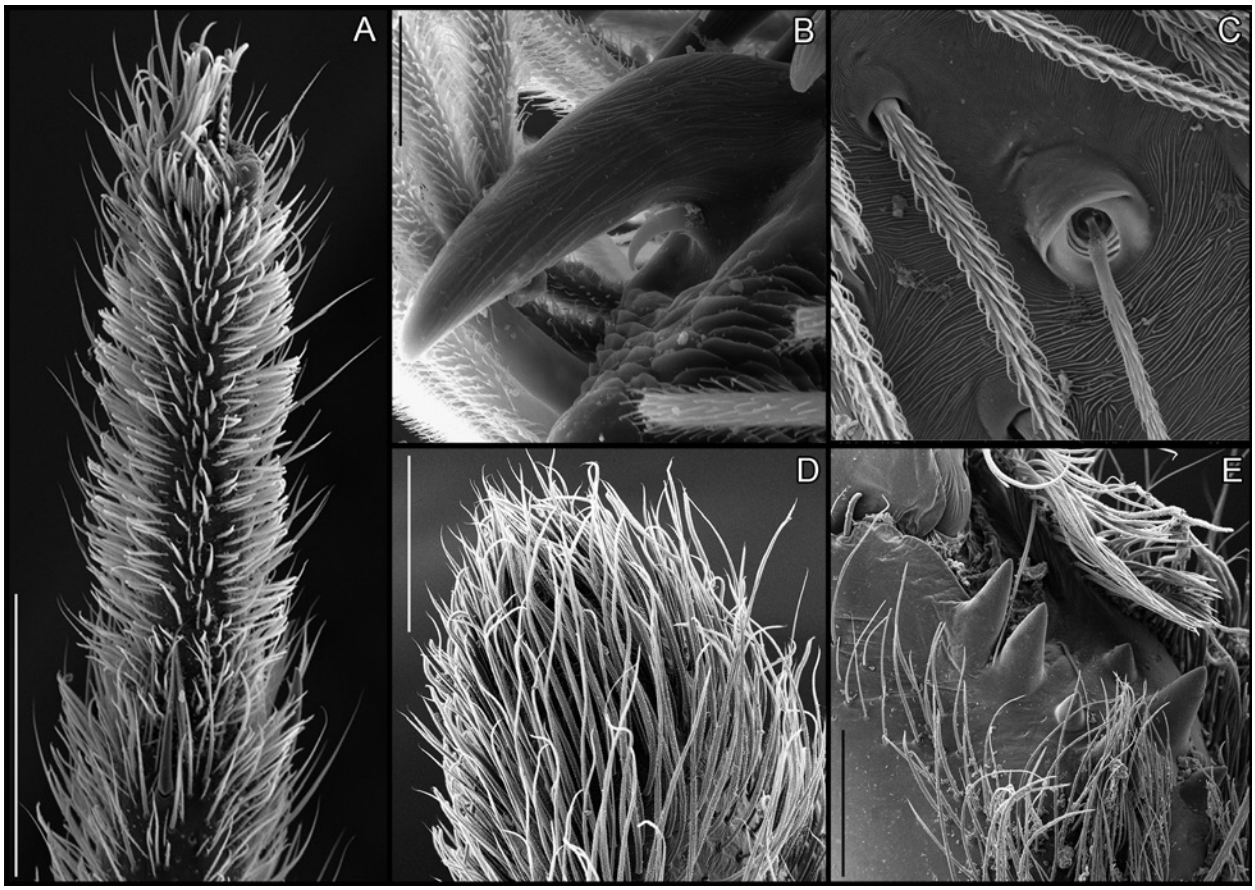

Fig. 4. *Diapontia uruguayensis* Keyserling **A**–**C** female, **D**,**E** male. **A**: Left tarsus of leg I, ventral view. **B**: Intertarsal claw left leg I. **C**: Trichobothrial socket. **D**: Tip of cymbium. **E**: Chelicera anterior view. — ***Scale bars***: A 0.50 mm; B,C 0.02 mm; D 0.20 mm; E 0.40 mm.

dorsal profile straight in lateral view. Carapace with two longitudinal submarginal pale bands enhanced by white setae (Fig. 10A), cephalic region narrowest in dorsal view, additionally in *D. niveovittata* and occasionally on *D. uruguayensis* there is a thin median pale band extending from the fovea to the PLER (Fig. 10C). Caput flanks gently sloping in frontal view, AER slightly procurved, somewhat wider than PMER but narrower than PLER, ALE disposed on small tubercles. Sternum longer than wide, reddish or yellowish-brown: *D. uruguayensis*, *D. niveovittata* and *D. anfibia* usually have a darker median band, also with dark areas opposing the coxae juntions (Fig. 10J). Chelicerae robust, reddish-brown or brown with three promarginal and three retromarginal teeth of the same size. Labium and endites yellowish brown or brown. Legs uniform light yellow-brown (Fig. 10J) to yellowish brown with darker areas (Fig. 16H), leg formula IV-I-II-III or IV-I-III-II. Tarsi with dense scopula, metatarsi I and II with weak scopula on the distal end (Fig. 4A). Tarsus with three claws, intertarsal claw with a single tooth (Fig. 4B). Abdomen ovoid, cardiac area usually marked, and two lines of white setae, either continuous or formed by spots (Fig. 10D), sometimes with broad light yellow-brown bands (Fig. 10B) or without any mark (Fig. 16E). Lateral margins of the abdomen uniform except in *D. uruguayensis*, *D. niveovittata* and *D. anfibia* which have numerous tufts of white setae ventrally yellowish brown (Fig. 16I), sometimes with obscure bands from the epigastric furrow to the spinnerets (Fig. 10I). Colulus as a fleshy triangular lobe, with several setae. The spinnerets have a similar conformation to that reported for other Lycosidae species (Santos & Brescovit 2001; Townley & Tillinghast 2003; Dolej et al. 2014; Piacentini 2014): ALS and PLS two-segmented, basal segment of PLS elongated (Fig. 3A). Anterior lateral spinnerets with two major ampullate gland spigots on the mesal margin (the posterior one reduced to a nubbin in the male) and about 60 piriform gland spigots (Fig. 3B). Posterior median spinnerets with aciniform and cylindrical gland spigots (absent in male), with a few setae between them, one minor ampullate gland spigot with a nubbin and a tartipore close to it PMS (Fig. 3C) with about 30 aciniform and six cylindrical gland spigots (absent in male), with few setae among them. Female PMS with two minor ampullate gland spigots with a tartipore close to them on the PMS (Fig. 3C) and only one minor ampullate gland spigot in the male. Posterior lateral spinnerets long, tubular, distal segment short, conical, with aciniform and cylindrical gland spigots (absent in male), with setae among them (Fig. 3D).

Palp of males with tibia longer than wide, without any apophysis or stridulatory organ, cymbium longer than the tibia, without macrosetae on its tip (Fig. 4D); conductor and lateral apophysis of the conductor fused, arising from

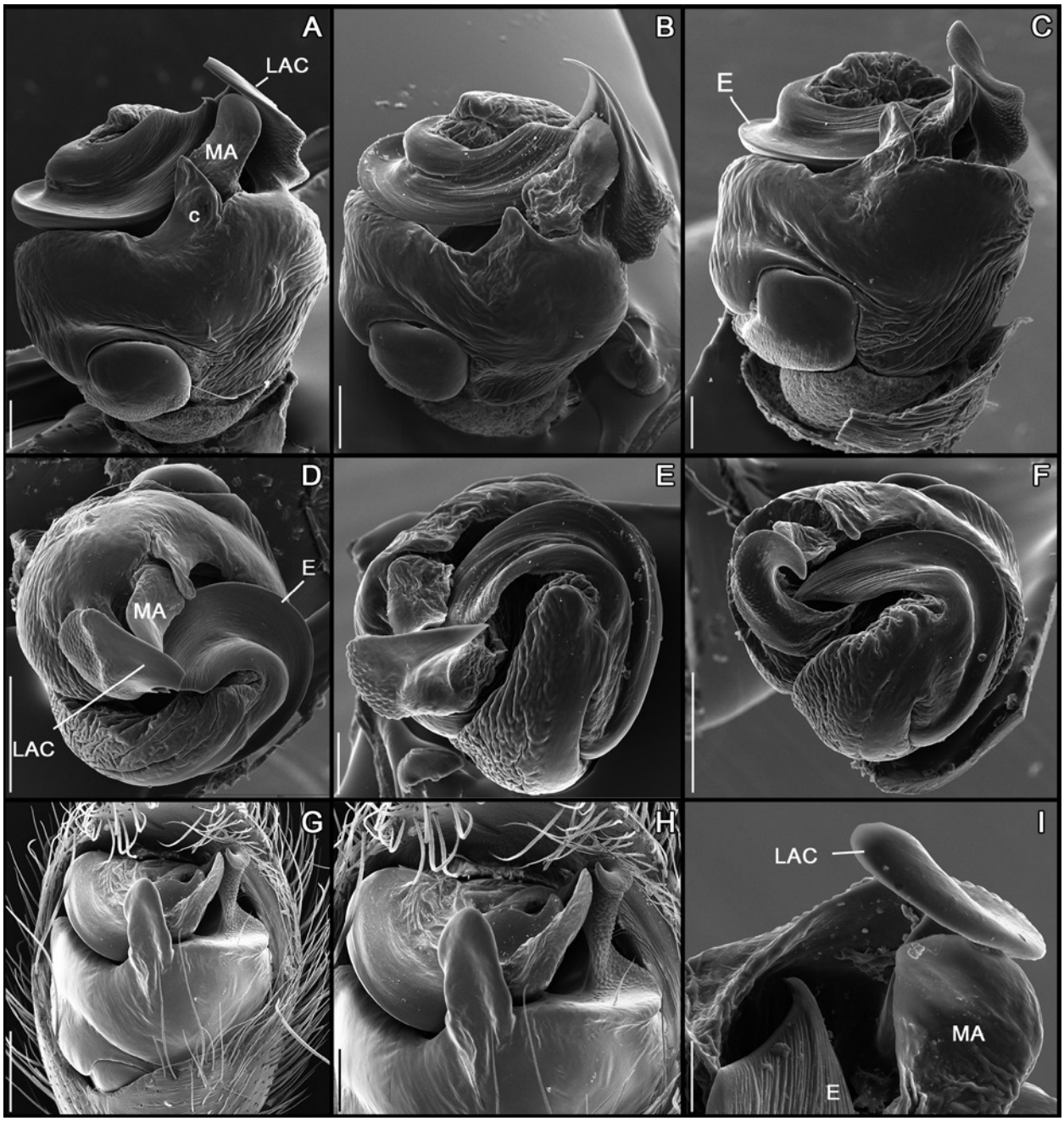

Fig. 5. Male genitalia. **A**,**D**: *Diapontia uruguayensis* Keyserling. **B**,**E**: *Diapontia niveovittata* Mello-Leitão. **C**,**F**,**I:** *Diapontia anfibia* (Zapfe-Mann) **comb.n. G**,**H**: *Diapontia securifera* (Tullgren) **comb.n. A**–**C**,**G**,**H**: Ventral view. **D**–**F**: Apical view. **I**: Retrolateral view. — ***Abbreviations***: c, ventral projection of tegulum; E, embolus; LAC, lateral apophysis of conductor; MA, median apophysis. — ***Scale bars***: A–C,F,H 0.20 mm; D,E 0.50 mm; G 0.40 mm; I 0.10 mm.

the retrolateral side of the bulb, with a rugose surface on the retrolateral and dorsal sides (Fig. 7C,D). Median apophysis laminar, poorly developed and retrolaterally (Fig. 7A–C) or longitudally directed (Fig. 13B). The ventral section of the bulb has an outgrowth of the tegular wall (Fig. 7B), labeled as apophysis c as in Sierwald (2000). Embolic division without apophysis, embolus C-shaped, pars pendula developed (Fig. 7B).

Epigyne of the female with a well-developed septum of different shapes, with lateral projections on *D. uruguayensis* (Fig. 7F) and *D. anfibia* (Fig. 9G). Atria shallow (Fig. 7F) or deep (Fig. 15D), limiting with bracket-like lateral lobes (Fig. 9G), the vulval chamber can be observed due to the transparency of the lateral lobes (Fig. 9G). Vulvar chamber developed (Fig. 7G), connected to the base of the spermatheca, stalk of the spermatheca usually short and straight, head of the spermatheca of the same width as the stalk, recognized by its pores (Fig. 18E). Bennet's gland present (Fig. 6G).

Distribution. Peru, Bolivia, Chile, southern Brazil, Paraguay, Uruguay and Argentina (Fig. 20).

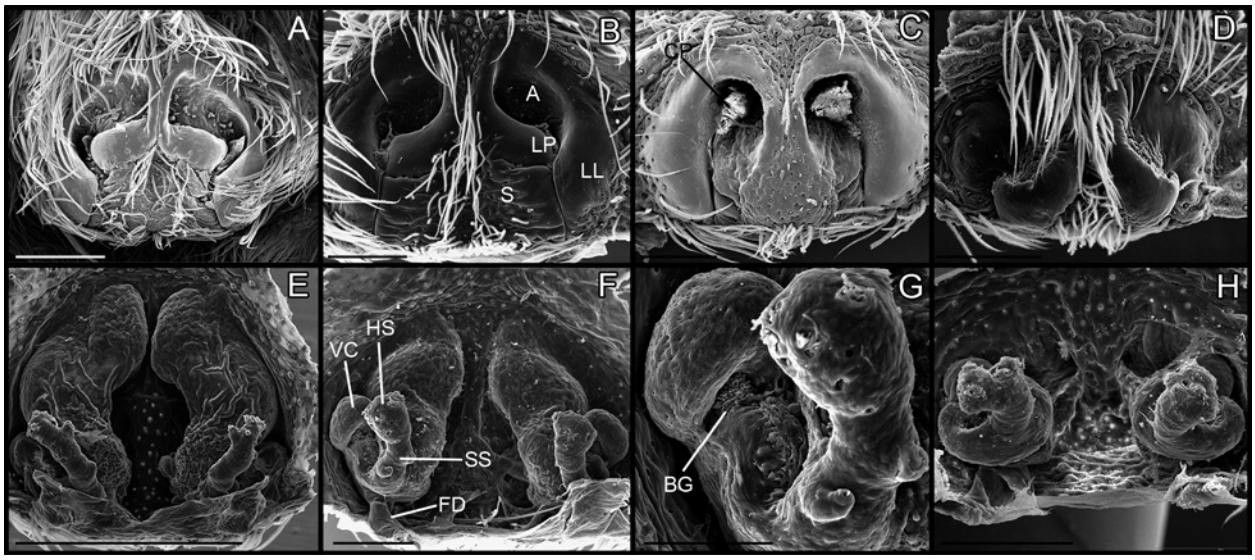

Fig. 6. Female genitalia. **A**,**E**: *Diapontia uruguayensis* Keyserling. **B**,**F**,**G**: *Diapontia anfibia* (Zapfe-Mann) **comb.n. C**: *Diapontia securifera* (Tullgren) **comb.n. D**,**H**: *Diapontia oxapampa* **sp.n. A**–**D**: Epigyne, ventral view. **D**–**H**: Vulva, dorsal view. — ***Abbreviations***: A, atrium; BG, Bennet's gland; CP, copulatory plug; FD, fertilization ducts; HS, head of spermatheca; LL, lateral lobes of epigyne; LP, lateral projections of septum; S, septum; SS, stalk of spermatheca; VC, vulval chamber. — ***Scale bars***: B,C,D,F,H 0.20 mm; G 0.10 mm; A 0.30 mm; E 0.50 mm.

3.3.2. *Diapontia uruguayensis* Keyserling, 1877

Figs. 4, 5A,D, 6A,E, 7, 10A,B,G–H, 11B–D, 20

Diapontia uruguayensis Keyserling, 1877: 675, plate 8, fig. 48.
Lycosa uruguayensis: Simon 1898: 347.
Tarentula uruguayensis: Strand 1908: 255 (likely a misidentification, see remark below).
Diapontia pourtaleensis Mello-Leitão, 1944: 341, fig. 30. **Syn.n.**
Diapontia senescens Mello-Leitão, 1944: 342, fig. 31. **Syn.n.**
Diapontia albopunctata Mello-Leitão, 1941: 123, fig. 20, plate 4, fig. 15. **Syn.n.**
Trochosa albopunctata: Roewer 1955: 301.
Diapontia infausta Mello-Leitão, 1941: 123, fig. 21, plate 4, fig. 16. **Syn.n.**
Trochosa infausta: Roewer 1955: 301.

Remarks. Strand (1908) described males and females of *D. uruguayensis* from Guaqui, Peru (currently Bolivia); at the end of the description, the author notes that the female epigyne had some differences to that described by Keyserling (1877), but considered these differences as a consequence of secretions. Since these specimens were destroyed during the World War II (in letter from Otto Kraus to María E. Galiano, November 1983), and there are no other records of *D. uruguayensis* from Guaqui or nearby localities, we consider it unlikely that the specimens examined by Strand were *D. uruguayensis*, but probably *D. securifera* that are morphologically similar and occur in nearby localities.

Differential diagnosis. Males of *Diapontia uruguayensis* resemble those of *D. anfibia* and *D. niveovittata* by the embolus running almost perpendicular to the longitudinal axis of the bulb on retrolateral view (Figs. 7A, 8A, 9A) and females by the presence of lateral projections on the septum (reduced on *D. niveovittata*); males can be differentiated by those of *D. anfibia* by the straight shape of the LAC (Figs. 5D, 7E) and from *D. niveovittata* by the elongated apophysis c (Fig. 7B). Females differ from those of *D. anfibia* by the absence of the incision on the septum (Figs. 6A, 7F) and from *D. niveovittata* in the lateral projections of the septum (Figs. 6A, 7F).

Synonymy. The holotype female of *D. uruguayensis* was compared with the type of *Diapontia pourtaleensis* Mello-Leitão, 1944, *D. senescens* Mello-Leitão, 1944, *D. albopunctata* Mello-Leitão, 1941 and *D. infausta* Mello-Leitão, 1941 and showed no significant morphological differences.

Description. ***Male* (*MACN-Ar 31393*)**: Carapace brown with pale submarginal bands, radial pattern indistinct (Fig. 10B). Sternum light yellow-brown, with a dark brown longitudinal median band and irregular dark marks opposing the coxae junctions (Fig. 10H). Labium and endites light yellow-brown (Fig. 10H). Chelicerae light yellow-brown; covered with brown bristles. Abdomen dark brown with two parallel longitudinal white bands, venter light yellow-brown with two central dark bands (Fig. 10H). Lateral margins of the abdomen with numerous tufts of white setae. Legs light yellow-brown without annulations.

Pedipalp as in Fig. 7A–E. Subtegulum small, located medially on the resting bulb. Tegulum large with a well-developed conductor, fused with the lateral apophysis (Fig. 7C, LAC). Lateral apophysis of the conductor triangular in apical view, with rounded tip (Fig. 7E). Apophysis c triangular (Fig. 7B, c). Median apophysis laminar, longitudinally directed (Fig. 7B, MA); sperm duct with an S-shaped trajectory in retrolateral view; embolic division without apophysis (Fig. 7E); embolus C-shaped with pars pendula well-developed (Fig. 7E, Pp).

Leg formula 4123. Spination pattern: femora **I p** 0-0-0-d2 **d** 1-0-1-1 **r** 0-1-0-1, **II p** 0-1-0-1 **d** 1-0-1-1 **r** 0-1-

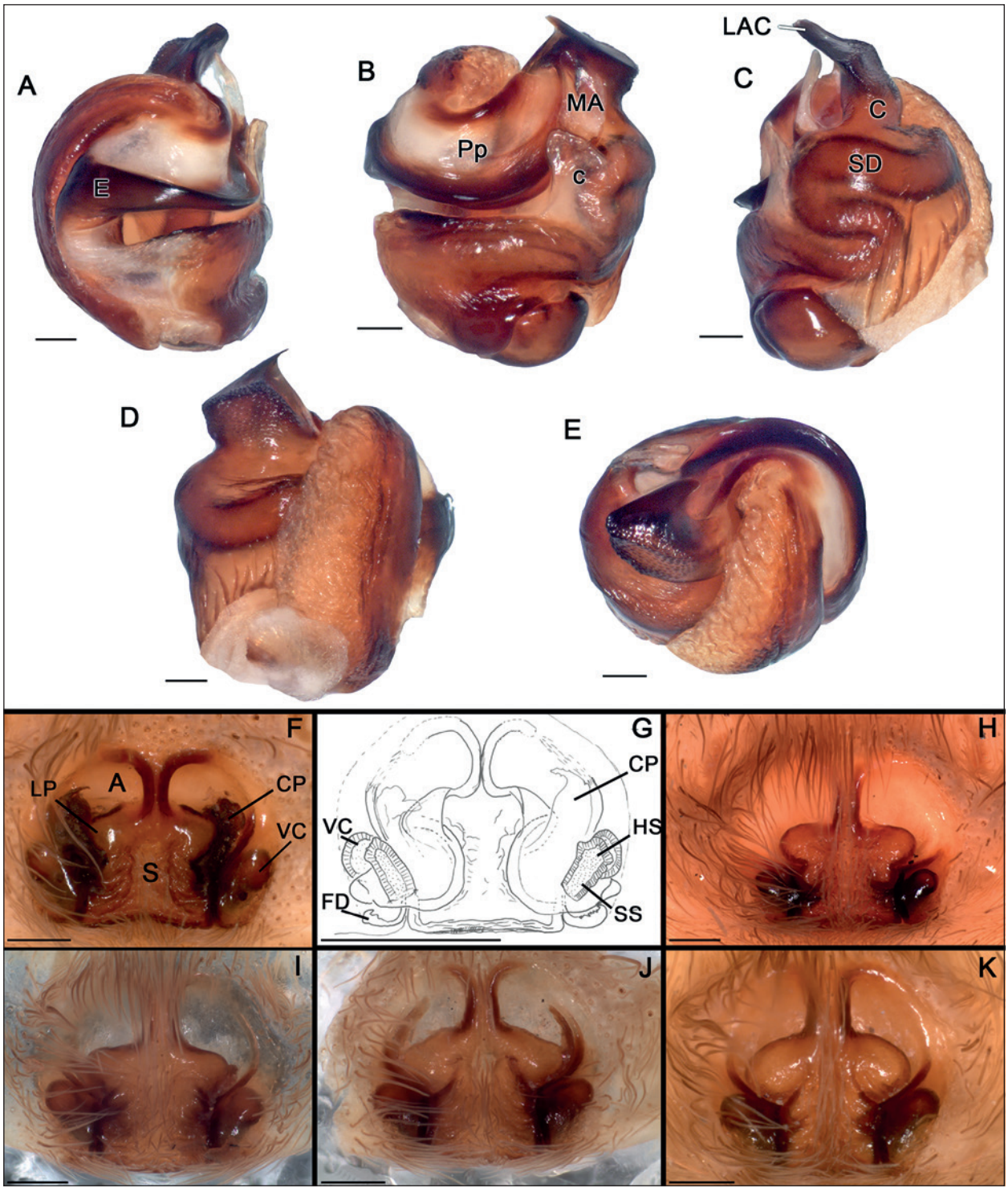

Fig. 7. *Diapontia uruguayensis* Keyserling, genitalia. **A**–**E**: Male bulb (MACN-Ar 31393): **A** prolateral; **B** ventral; **C** retrolateral; **D** dorsal; **E** apical. **F**: Epigyne ventral (FCE 3866). **G**: Vulva (FCE 3866). **H**: Epigyne ventral (MACN-Ar 23523). **I**: Epigyne ventral (MACN-Ar 7765). **J**: Epigyne ventral (MACN-Ar 7766). **K**: Epigyne ventral (FCE 3867). — ***Abbreviations***: A, atrium; C, conductor; c, ventral projection of tegulum; CP, copulatory plug; E, embolus; FD, fertilization ducts; HS, head of spermatheca; LAC, lateral apophysis of conductor; MA, median apophysis; S, septum; SS, stalk of spermatheca; VC, vulval chamber. — ***Scale bars***: A–F,H–K 0.20 mm; G 0.50 mm.

0-1, **III p** 0-1-0-1 **d** 1-0-1-1 **r** 0-1-0-1, **IV p** 0-1-0-1 **d** 1-0-1-1 **r** 0-0-0-1; patellae **I p** 1 **r** 1, **II p** 1 **r** 1, **III p** 1 **r** 1, **IV p** 1 **r** 1; tibiae **I p** d1-d1 **r** d1-d1 **v** 2-2-2ap, **II p** d1-d1 **d** 0-1 **r** d1-d1 **v** r1-2-2ap, **III p** d1-d1 **d** 1-1 **r** 1-1 **v** p1-2-2ap, **IV p** 1-1 **d** 1-1 **r** 1-1 **v** p1-2-2ap; metatarsi **I p** 1-1ap **r** 0-1ap **v** 2-2-3ap, **II p** 1-1-1ap **r** 1-1-1ap **v** 2-2-3ap, **III p** d1-d1-d1ap **r** d1-d1-d1ap **v** 2-2-3ap, **IV p** d1-d1-d1ap **r** d1-d1-d1ap **v** 2-2-3ap.

***Female* (*FCE 3866*)**: Carapace brown with pale submarginal bands, radial pattern indistinct (Fig. 10A). Sternum dark brown (Fig. 10G). Labium and endites brown (Fig. 10G). Chelicerae brown; covered with brown bris-

tles. Abdomen dark brown with two parallel longitudinal white bands, venter light yellow-brown with two central dark bands (Fig. 10A). Lateral margins of the abdomen with numerous tufts of white setae. Legs light yellow-brown without annulations.

Epigyne as in Fig. 7F, atria comma-shaped (Fig. 7F, A) septum broad with rounded lateral projections; copulatory openings located on or at lateral margins of the septum. Vulva as in Fig. 7F, head of spermathecae (Fig. 7G, HS) similar in width to the short and straight stalk, vulval chambers rounded (Fig. 7G, VC).

Leg formula 4123. Spination pattern: femora **I p** 0-0-0-d2 **d** 1-0-1-1 **r** 0-1-0-1, **II p** 0-1-0-1 **d** 1-0-1-1 **r** 0-1-0-1, **III p** 0-1-0-1 **d** 1-0-1-1 **r** 0-1-0-1, **IV p** 0-1-0-1 **d** 1-0-1-1 **r** 0-0-0-1; patellae **I r** 1, **II p** 1 **r** 1, **III p** 1 **d** 1-1 **r** 1, **IV p** 1 **d** 1-1 **r** 1; tibiae **I p** 0-d1 **v** 2-2-2ap, **II p** d1-d1 **v** p1-2-2ap, **III p** d1-d1 **d** 1-1 **r** 1-1 **v** p1-2-2ap, **IV p** d1-d1 **d** 1-1 **r** d1-d1 **v** p1-2-2ap; metatarsi **I p** 1-1ap **r** 0-1ap **v** 2-2-3ap, **II p** 1-1ap **r** 0-1ap **v** 2-2-3ap, **III p** 1-1-1ap **r** 1-1-1ap **v** 2-2-3ap, **IV p** 1-1-1ap **r** 1-1-1ap **v** 2-2-3ap.

Measurements: Female, FCE 3866 (male, MACN-Ar 31393): TL 9.58 (7.85), PL 4.93 (4.13), PW 3.93 (3.27), PH 1.87 (1.47), AL 5.33 (3.67). Eyes: AME 0.22 (0.17), ALE 0.18 (0.15), PME 0.32 (0.25), PLE 0.33 (0.27). Row of eyes: AER 1.08 (0.92), PMER 0.92 (0.77), PLER 1.42 (1.20). Sternum (length/width) 2.33/2.07 (1.93/1.60). Labium (length/width) 0.83/0.68 (0.55/0.58). Legs: length of segments (femur + patella/tibia + metatarsus + tarsus = total length): **I** 3.67 + 4.80 + 2.73 + 1.53 = 12.7, **II** 3.47 + 4.27 + 2.80 + 1.60 = 12.14, **III** 3.33 + 4.00 + 2.93 + 1.53 = 11.79, **IV** 4.53 + 5.93 + 4.33 + 2.07 = 16.86 (**I** 3.33 + 4.33 + 2.73 + 1.60 = 11.99, **II** 3.27 + 4.27 + 2.73 + 1.53 = 11.80, **III** 3.27 + 3.93 + 3.00 + 1.60 = 11.80, **IV** 4.27 + 5.07 + 4.67 + 2.07 = 16.08).

Variation: Female (male) (range, mean ± s.d.): TL 7.28–14.10, 10.28 ± 2.02; CL 3.68–5.99, 4.88 ± 0.65; CW 3.02–5.00, 3.85 ± 0.55; n = 10 (TL 6.09–10.70, 7.40 ± 1.47; CL 3.25–4.92, 3.88 ± 0.61; CW 2.43–3.95, 3.14 ± 0.46; n = 10). Some colour variation was recorded. The carapace of males and females can have occasionally a fine light median band enhanced by white setae and the sternum varies from dark brown to light yellow-brown, with a dark brown longitudinal median band and irregular dark marks opposite the base of each coxa. Some specimens have three retromarginal teeth on one chelicera and four on the other, or 4–4 (left–right); in only one case, we recorded 6–4. Variations in the shape of the median septum are illustrated in Fig. 7H–K.

Type material examined. HOLOTYPE of *D. uruguayensis* ♀, 'URUGUAY, 2010-19 | *Diapontia uruguayensis* type', (BMNH 2010-19). HOLOTYPE of *D. pourtaleensis* ♂, 'ARGENTINA, Buenos Aires, Pourtalé II-1941, M. Birabén leg.' | '16025', (MLP-16025). HOLOTYPE of *D. senescens* ♀, 'ARGENTINA, Buenos Aires, General Guido II-1941, M. Birabén leg' | '16030', (MLP-16030). HOLOTYPE of *D. albopunctata* ♀, 'ARGENTINA, Córdoba, Anisacate I-1939, M. Birabén leg.' '14675', (MLP-14675). HOLOTYPE of *D. infausta* ♀, 'ARGENTINA, Córdoba, Río Segundo' | '14676', (MLP-14676).

Other material examined. See Electronic Supplement File 1.

Distribution. Northern Paraguay (recorded from Concepción Province), southeastern Brazil (Rio Grande do Sul), southern Uruguay (Maldonado, Rocha and Canelones Provinces), southern to northeastern Argentina (Chaco, La Rioja, San Juan, San Luis, Córdoba, Entre Ríos, Buenos Aires, Neuquén and Chubut) and southern Chile (Aysén and Palena Provinces) (Fig. 20A).

Natural history. Many specimens were collected from marshy vegetation in open spaces. Females and immatures construct a funnel web between low vegetation or at ground level using holes in the mud as retreats (Fig. 11A–C). The web consists of a woven sheet with a funnel retreat leading into the ground or dense vegetation. Adult males and females are collected throughout the year, near water bodies, on webs or running over the water. Eggsacs were recorded in spring and summer; a female was collected with 93 spiderlings in April (MACN-Ar 34175) and another with 108 spiderlings in November (FCE 3866).

In August 2015 during floods in Paraje el Destino, Lezama (Buenos Aires Province) a mass accumulation of spiders covered the vegetation on the road embankment with a dense sheet of white silk. *Diapontia uruguayensis* was the second most abundant species following the lycosine *Alopecosa moesta* (Holmberg, 1876) in the samples, and we observed many specimens ballooning.

We observed four sexual encounters. In three cases the male tried to copulate without any courtship when it was introduced to the female container. In the fourth encounter the male began a courtship with short steps raising the abdomen and moving it from side to side and elevating both legs I. While approaching to the female the male moved the palps resembling pedaling. This kind of courtship was also observed in a male placed in an empty female cage, suggesting that chemical cues are involved, as is common in Lycosidae (Rypstra et al. 2003; Roberts & Uetz 2005). In two cases the male mounted the female from behind and tried to introduce the embolus in the epigyne from this position and then turned 180 degrees. In the other two cases the male mounted the female from the front and locking the first pair of legs of the female with its own legs (Fig. 11D), adopting the typical position described for lycosids (Farley & Shear 1973). The duration of copulations ranged from 1 hour and 42 minutes to 4 hours and 23 minutes. In the longest copulation the female became active five times and walked around with the male still on her dorsum; when the female stopped, the male touch the female with his legs I and II across the abdomen. After mating finished the females remained motionless for several minutes since the males move away. The insertions series (as defined in Rovner 1974) consisted of 67 insertions in the shortest encounter and 53 in the longest.

One month and seven days after mating, one of the females made an eggsac. The first step of the eggsac construction was a creation of a dense circular white silk platform over the sheet web; on this, she laid the eggs in two layers, and then covered the eggs with another circular dense white web. The female did this by stradd-

ling the eggs, with the palps touching the borders of the semicircular web and moving the abdomen from left to right, applying silk lines on the borders and then elevating the pedicelum and touching the opposite side of the web. Once the eggs were covered, the female started to cut the borders with the chelicerae, pulling the eggsac and picking up it with the legs III–IV. When the eggsac was almost released the female pulled very strongly, with the eggsac already attached to the spinnerets; as the eggsac did not release she turned the carapace and cut the attachment with the chelicerae. The leftover of the circular valves were bent by the female with the chelicerae and palps, all in the same direction. Once the eggsac was fully released from the web, the mother remained still for 18 minutes, then picked up the eggsac with the chelicerae and turned it upside down. The side of the eggsac that was facing up acquired an aquamarine colour (Fig. 12B). After ten minutes, the bottom half also become aquamarine; the only part that remained white was on the union of the two valves. The eggsac was lenticular in shape and about 6 mm in diameter; the next day the eggsac had a dark green colour (Fig. 12C).

3.3.3. *Diapontia niveovittata* Mello-Leitão, 1945

Figs. 3, 5B,E, 8, 10C,D,I,J, 11A, 12B,C, 20A

Diapontia niveovittata Mello-Leitão, 1945: 248.

Remarks. MELLO-LEITÃO (1945) described this species based on one male and one female from Curuzu Cuatiá, Corrientes, without providing illustrations or description of the genitalia and indicating that the specimens were deposited on the Museo de La Plata in the vial MLP 14490. We examined the vial and found only a subadult male in very bad condition, with the carapace, appendages and abdomen separated. We recognize this species through material collected near the type locality and the original description.

Differential diagnosis. Males of *Diapontia niveovittata* resemble those of *D. anfibia* and *D. uruguayensis* by the embolus running almost perpendicular to the longitudinal axis of the bulb in retrolateral view (Figs. 7A, 8A, 9A) and females by the broad and shallow atria (Fig. 7F, 8F, 9F); males can be differentiated by small apophysis c (Figs. 5B, 8B) and females by the reduction of the lateral projections of the septum (Fig. 8F).

Description. ***Male* (*MACN-Ar 28793*)**: Carapace brown with a fine light median band enhanced by white setae and pale submarginal bands, radial pattern indistinct (Fig. 10D). Sternum pale, with a dark brown longitudinal median band and irregular dark marks opposite to the base of the coxae (Fig. 10J). Labium and endites light yellow-brown (Fig. 10J). Chelicerae light yellow-brown; covered with brown bristles. Dorsum of abdomen dark brown with two parallel longitudinal white bands (Fig. 10D), venter light yellow-brown with two central dark bands (Fig. 10J). Lateral margins of the abdomen with numerous tufts of white setae. Legs light yellow-brown without annulations.

Pedipalp as in Fig. 8A–E. Subtegulum small, located medially on the resting bulb. Tegulum large with a well-developed conductor, fused apically with the lateral apophysis (Fig. 8C, LAC), lateral apophysis of the conductor triangular in apical view, with an acute tip (Fig. 8E). Apophysis c as a small tegular projection (Fig. 8B). Median apophysis laminar, longitudinally directed (Fig. 8B, MA); sperm duct with an S-shaped trajectory in retrolateral view; embolic division without apophysis (Fig. 8C, SD); embolus with pars pendula (Fig. 8C, Pp).

Leg formula 4132. Spination pattern: femora **I p** 0-0-0-d2 **d** 1-0-1-1 **r** 0-1-0-1, **II p** 0-1-0-1 **d** 1-0-1-1 **r** 0-1-0-1, **III p** 0-1-0-1 **d** 1-0-1-1 **r** 0-1-0-1, **IV p** 0-1-0-1 **d** 1-0-1-1 **r** 0-0-0-1; patellae **I r** 1, **II p** 1 **r** 1, **III p** 1 **r** 1, **IV p** 1 **r** 1; tibiae **I p** 0-d1 **v** 2-2-2ap, **II p** d1-d1 **v** 2-2-2ap **r** d1-d1, **III p** d1-d1 **d** 1-1 **r** 1-1 **v** 2-2-2ap, **IV p** d1-d1 **d** 1-1 **r** d1-d1 **v** 2-2-2ap; metatarsi **I p** 1-1ap **r** 0-1ap **v** 2-2-3ap, **II p** 1-1ap **r** 1-1ap **v** 2-2-3ap, **III p** 1-1ap **r** 1-1ap **v** 2-2-3ap, **IV p** 1-1ap **r** 1-1ap **v** 2-2-3ap.

***Female* (*MACN-Ar 13301*)**: Colour in ethanol as in male (Fig. 10C,I).

Epigyne as in Fig. 8F, septum triangular shape without projections; copulatory openings located on or at lateral margins of the septum. Vulva as in Fig. 8G, head of spermathecae (Fig. 8G, HS) similar in width to the short and straight stalk, vulval chambers rounded (Fig. 8G, VC).

Leg formula 4132. Spination pattern: femora **I p** 0-0-0-d2 **d** 1-0-1-1 **r** 0-1-0-1, **II p** 0-1-0-1 **d** 1-0-1-1 **r** 0-1-0-1, **III p** 0-1-0-1 **d** 1-0-1-1 **r** 0-1-0-1, **IV p** 0-1-0-1 **d** 1-0-1-1 **r** 0-0-0-1; patellae **II p** 1, **III p** 1 **r** 1, **IV p** 1 **r** 1; tibiae **I p** 0-d1 **v** 2-2-2ap, **II p** d1-d1 **v** 2-2-2ap **r** 0-d1, **III p** d1-d1 **d** 1-1 **r** 1-1 **v** p1-2-2ap, **IV p** d1-d1 **d** 1-1 **r** d1-d1 **v** p1-2-2ap; metatarsi **I p** 0-1ap **r** 0-1ap **v** 2-2-3ap, **II p** d1-1ap **r** 0-1ap **v** 2-2-3ap, **III p** 0-1ap **r** 0-1ap **v** 2-2-3ap, **d** 2-2-1ap, **IV d** 2-2-2ap, **v** 2-2-3ap.

Measurements: Male, MACN-Ar 28793 (Female, MACN-Ar 13301): TL 7.32 (8.91), PL 3.73 (4.67), PW 2.87 (3.60), PH 1.47 (1.67), AL 3.27 (4.13). Eyes: AME 0.15 (0.20), ALE 0.13 (0.17), PME 0.32 (0.30), PLE 0.23 (0.27). Row of eyes: AER 0.85 (1.25), PMER 0.73 (0.93), PLER 1.33 (1.42). Sternum (length/width) 2.07/1.53 (2.47/2.00). Labium (length/width) 0.58/0.55. (0.75/0.72) Legs: length of segments (femur + patella/tibia + metatarsus + tarsus = total length): **I** 2.93 + 3.93 + 2.40 + 1.53 = 10.79, **II** 2.80 + 3.73 + 2.47 + 1.40 = 10.40, **III** 3.07 + 3.53 + 2.73 + 1.40 = 10.73, **IV** 3.60 + 4.73 + 3.87 + 1.93 = 14.13 (**I** 4.00 + 5.00 + 3.00 + 1.67 = 13.67, **II** 3.47 + 5.20 + 2.87 + 1.60 = 13.14, **III** 3.33 + 4.07 + 3.07 + 1.40 = 11.87, **IV** 4.67 + 5.87 + 4.80 + 2.13 = 17.47).

Variation: Male (female) (range, mean ± s.d.): TL 6.52–7.32, 6.86±0.29; CL 2.87–3.33, 3.45±0.17; CW 2.53–2.87, 2.71±0.13; n=6 (TL 8.91–10.91, 9.58±1.15; CL 4.67–5.40, 4.98±0.38; CW 3.60–4.13, 3.84±0.27; n = 10).

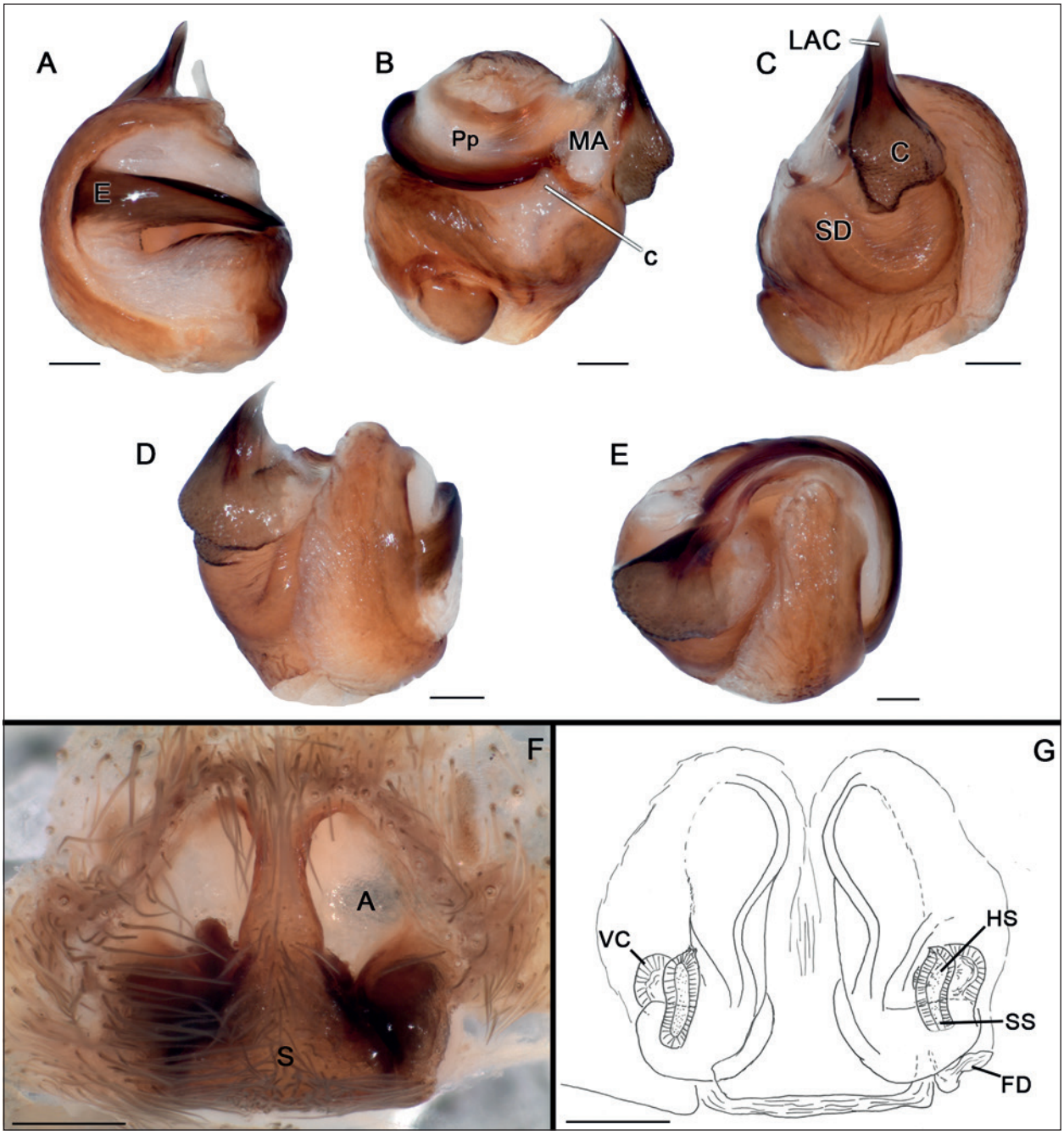

Fig. 8. *Diapontia niveovittata* Mello-Leitão, genitalia. **A**–**E**: Male bulb (MACN-Ar 30520): **A** prolateral; **B** ventral; **C** retrolateral; **D** dorsal; **E** apical. **F**: Epigyne ventral (MACN-Ar 28615). **G**: Vulva (MACN-Ar 28615). — ***Abbreviations***: A, atrium; C, conductor; c, ventral projection of tegulum; E, embolus; FD, fertilization ducts; HS, head of spermatheca; LAC, lateral apophysis of conductor; MA, median apophysis; S, septum; SS, stalk of spermatheca; VC, vulval chamber. — ***Scale bars***: 0.20 mm.

Type material examined. SYNTYPE of *D. niveovittata* subadult male, 'ARGENTINA, Corrientes, Curuzú-Cuatiá, XI-1941, M. Birabén leg.' | '14490', (MLP 14490).

Other material examined. See Electronic Supplement File 1.

Distribution. Southern Paraguay (Asunción), North-Central Argentina (Salta, Formosa, Corrientes, Santa Fe, San Juan, Entre Ríos and Buenos Aires Provinces) and southern Brazil (São Paulo) (Fig. 20A).

Natural history. Most specimens were collected in funnel webs similar to those of *D. uruguayensis* or running over the water surface. Adult males and females were collected throughout the year, females with eggsac were recorded in spring, summer and autumn. One female was collected with 115 spiderlings in autumn.

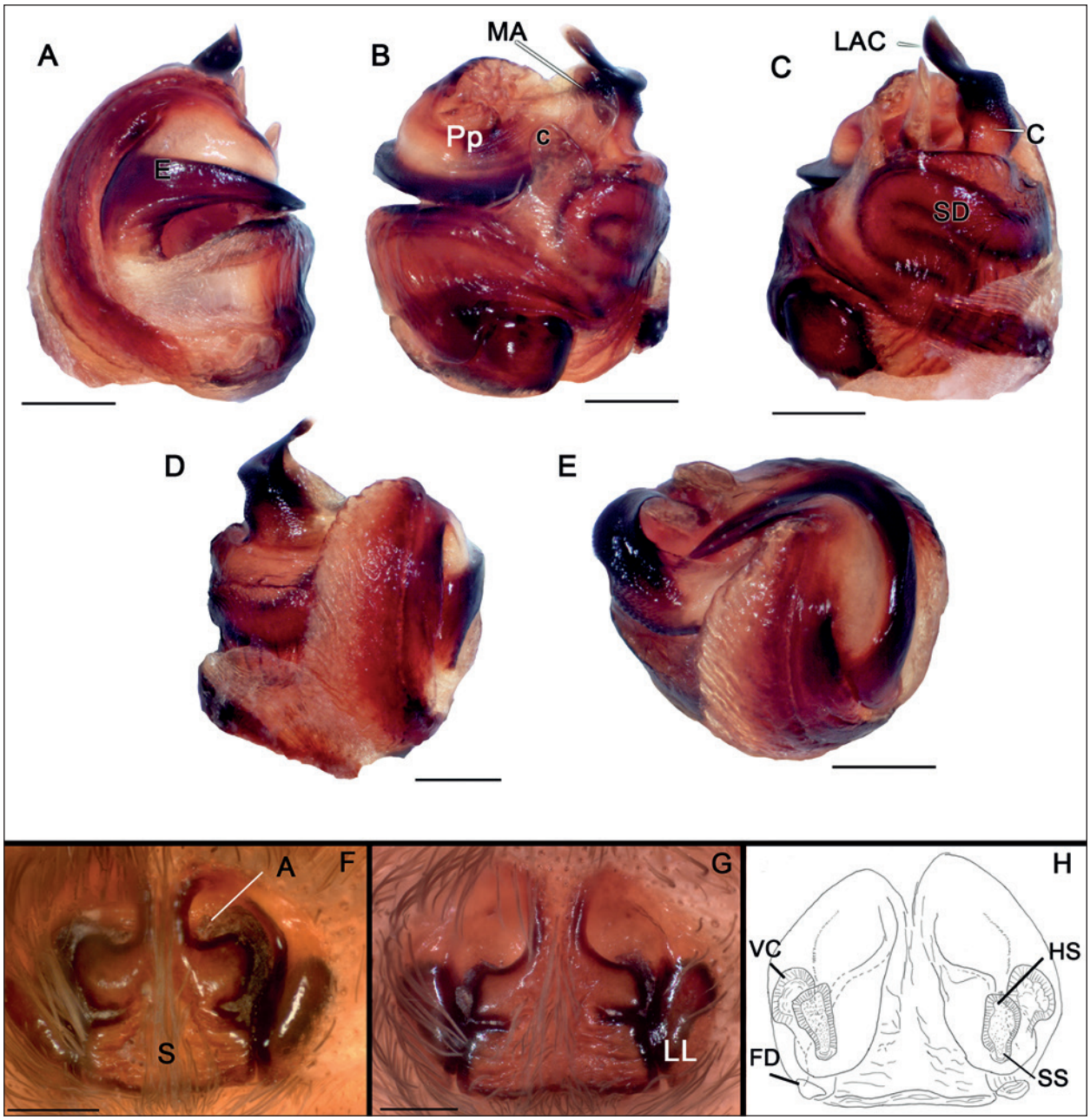

Fig. 9. *Diapontia anfibia* (Zapfe-Mann) **comb.n.**, genitalia. **A**–**E**: Male bulb (male from Concepción, Chile; AMNH): **A** prolateral; **B** ventral; **C** retrolateral; **D** dorsal; **E** apical. **F**: Epigyne ventral (female from Concepción, Chile AMNH). **G**: Epigyne ventral (female from Concepción, Chile AMNH). **H**: vulva (female from Concepción, Chile AMNH). — ***Abbreviations***: A, atrium; C, conductor; c, ventral projection of tegulum; E, embolus; FD, fertilization ducts; HS, head of spermatheca; LAC, lateral apophysis of conductor; LL, lateral lobes of epigyne; MA, median apophysis; S, septum; SS, stalk of spermatheca; VC, vulval chamber. — ***Scale bars***: 0.20 mm.

3.3.4. *Diapontia anfibia* (Zapfe-Mann, 1979) comb.n.

Figs. 5C,F,I, 6B,F,G, 12A, 9, 10E,F,K,L, 20A

Pardosa anfibia Zapfe-Mann, 1979: 3, figs. 3, 4.
Lycosa artigasi Casanueva, 1980: 25, figs. 22–25. **Syn.n.**

Differential diagnosis. Males of *Diapontia niveovittata* resemble those of *D. anfibia* and *D. uruguayensis* by the embolus running almost perpendicular to the longitudinal axis of the bulb in retrolateral view (Figs. 7A, 8A, 9A) and females by the broad and shallow atria (Figs. 7F, 8F, 9F); males can be differentiated by the hook-like lateral apophysis of the conductor (Figs. 5F, 9F) and females by the deep lateral incisions in the septum (Figs. 6B, 9G).

Synonymy. The holotype female of *D. anfibia* was compared with the type of *Lycosa artigasi* Casanueva, 1980 and show no significant morphological differences.

Description. ***Male from Concepción Province, Río Andalien (AMNH)***: Carapace brown with pale submarginal bands, radial pattern indistinct (Fig. 10F). Sternum, la-

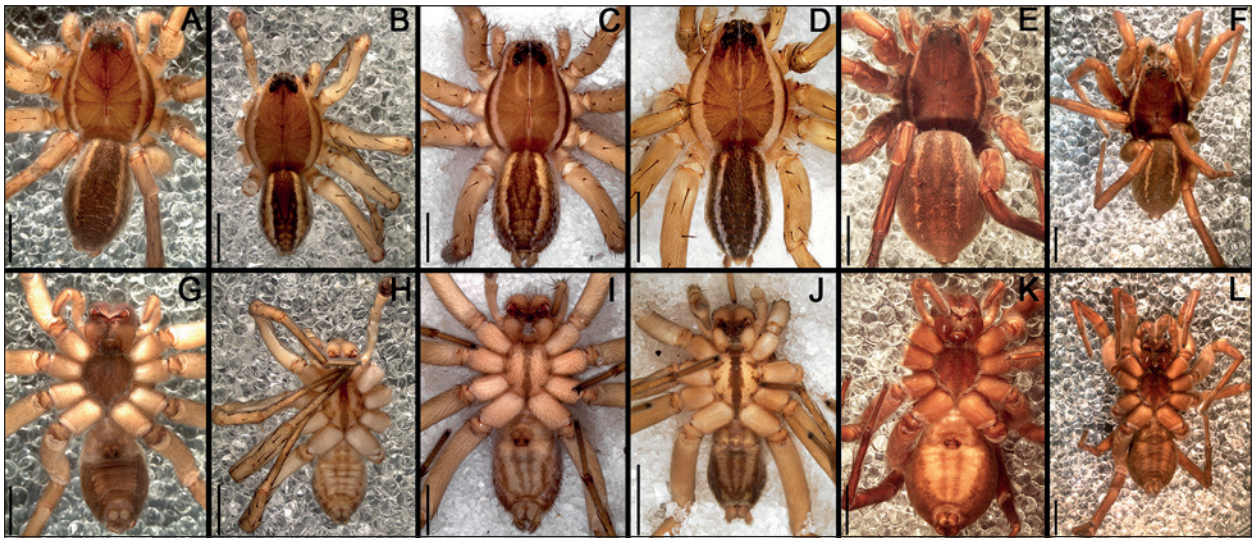

Fig. 10. Habitus, **A**–**F** dorsal; **G**–**L** ventral. **A**,**B**,**G**,**H**: *Diapontia uruguayensis* Keyserling. **A**,**G** female; **B**,**H** male. **C**,**D**,**I**,**J**: *Diapontia niveovittata* Mello-Leitão. **C**,**I** female; **D**,**J** male. **E**,**F**,**K**,**L**: *Diapontia anfibia* (Zapfe-Mann) **comb.n. E**,**K** female; **F**,**L** male. — ***Scale bars***: 2.00 mm.

bium and endites dark brown (Fig. 10L). Chelicerae light yellow-brown; covered with brown bristles. Abdomen dark brown with two parallel longitudinal thin white bands (Fig. 10F), venter dark brown with two central light yellow-brown bands (Fig. 10L). Legs brown with some paler areas.

Pedipalp as in Fig. 9A–E. Subtegulum small, located medially in the resting bulb. Tegulum large with a well-developed conductor, fused apically with the lateral apophysis (Fig. 9C, LAC), lateral apophysis of the conductor hook-like in apical view (Fig. 9E). Apophysis c triangular (Fig. 9B, c). Median apophysis laminar and longitudinally directed (Fig. 9B, MA); sperm duct with an S-shaped trajectory in retrolateral view (Fig. 9C, MA); embolic division without apophysis (Fig. 9E); embolus with pars pendula (Fig. 9B, Pp).

Leg formula 4123. Spination pattern: femora **I p** 0-0-0-d2 **d** 1-0-1-1 **r** 0-1-0-1, **II p** 0-1-0-1 **d** 1-0-1-1 **r** 0-1-0-1, **III p** 0-1-0-1 **d** 1-0-1-1 **r** 0-1-0-1, **IV p** 0-1-0-1 **d** 1-0-1-1 **r** 0-0-0-1; patellae **II p** 1, **III p** 1 **r** 1, **IV p** 1 **r** 1; tibiae **I p** 0-d1 **v** 2-2-2ap, **II p** d1-d1 **v** 2-2-2ap **r** 0-d1, **III p** d1-d1 **d** 1-1 **r** 1-1 **v** p1-2-2ap, **IV p** d1-d1 **d** 1-1 **r** d1-d1 **v** p1-2-2ap; metatarsi **I p** 1-1ap **v** 2-2-3ap, **II p** 1-1ap **r** 1-1ap **v** 2-2-3ap, **III p** 1-1ap **r** 1-1ap **v** 2-2-3ap, **IV p** 1-1ap **r** 1-1ap **v** 2-2-3ap.

***Female* (*same data as male*)**: Colour in ethanol as in male (Fig. 10E,K).

Epigyne as in Fig. 9G, atria in the shape of comma septum board with a deep middle incision and rectangular lateral projections; copulatory openings located on or at lateral margins of the septum. Vulva as in Fig. 9H, head of spermatheca (Fig. 9H, HS) similar in width to the short and straight stalk, vulval chambers rounded (Fig. 9H, VC).

Leg formula 4123. Spination pattern: femora **I p** 0-0-0-d2 **d** 1-0-1-1 **r** 0-1-0-1, **II p** 0-1-0-1 **d** 1-0-1-1 **r** 0-0-0-1, **III p** 0-1-0-1 **d** 1-0-1-1 **r** 0-1-0-1, **IV p** 0-1-0-1 **d** 1-0-1-1 **r** 0-0-0-1; patellae **II p** 1, **III p** 1 **r** 1, **IV p** 1 **r** 1; tibiae **I v** 2-2-2ap, **II p** d1-d1 **v** 2-2-2ap, **III p** d1-d1 **d** 1-1 **r** 1-1 **v** p1-p1-2ap, **IV p** d1-d1 **d** 1-1 **r** d1-d1 **v** p1-2-2ap; metatarsi **I v** 2-2-3ap, **II p** 1-1ap **v** 2-2-3ap, **III p** d1-1-1ap **r** d1-1-1ap **v** 2-2-3ap, **IV p** 1-1-1ap **r** 1-1-1ap **v** 2-2-3ap.

Measurements: Male (female): TL 9.44 (10.37), PL 4.67 (4.67), PW 3.60 (3.67), PH 1.60 (1.73), AL 4.60 (5.33). Eyes: AME 0.22 (0.18), ALE 0.18 (0.17), PME 0.28 (0.25), PLE 0.32 (0.28). Row of eyes: AER 1.03 (1.12), PMER 0.93 (0.93), PLER 1.37 (1.33). Sternum (length/width) 2.27/1.93 (2.33/1.87). Labium (length/width) 0.68/0.65 (0.70/0.67). Legs: length of segments (femur + patella/tibia + metatarsus + tarsus = total length): **I** 3.47 + 4.33 + 2.60 + 1.47 = 11.87, **II** 3.40 + 4.00 + 2.47 + 1.47 = 11.34, **III** 3.33 + 3.67 + 2.60 + 1.40 = 11.00, **IV** 3.93 + 4.40 + 4.00 + 2.00 = 14.33 (**I** 3.13 + 4.07 + 2.27 + 1.40 = 10.87, **II** 3.27 + 3.80 + 2.33 + 1.40 = 10.80, **III** 2.80 + 3.67 + 2.40 + 1.40 = 10.27, **IV** 3.87 + 4.67 + 3.67 + 1.93 = 14.14).

Variation: Male (female) (range, mean ± s.d.): TL 6.65–9.44, 7.74 ± 0.92; CL 2.93–4.73, 3.99 ± 0.58; CW 2.00–3.80, 3.00 ± 0.53; n = 10 (TL 9.31–13.30, 10.63 ± 1.36; CL 4.27–5.67, 4.90 ± 0.39; CW 3.20–4.67, 3.79 ± 0.41; n = 10). The shape of the lateral projections of the epigynal septum has some variations (Fig. 9F).

Type material examined. HOLOTYPE of *D. anfibia* ♂ 'Pardosa anfibia Isla de Maipo 17-iv-1977' | 'M.N.H.N. Tipo Nº 3618' | 'HOLOTIPO', PARATYPES of *D. anfibia* 5 ♂ and 6 ♀ in 11 vials each vial with a label 'Isla de Maipo 17-iv-1977', males with a label 'Pardosa anfibia ♂ Zapfe 1979', females with a label 'Pardosa anfibia ♀ Zapfe 1979' and each vial with a label 'M.N.H.N. Tipo Nº' with numbers from 3619 to 3624 with one female and 3625 to 3628 with one male each. HOLOTYPE of *L. artigasi* ♂ 'CHILE, Región de la Araucanía, Provincia de Malleco, Parque Nacional Tolhuaca, Laguna Malleco' (MHNC).

Other material examined. See Electronic Supplement File 1.

Fig. 11. Live specimens. **A**: *Diapontia niveovittata* Mello-Leitão from Corrientes, Argentina, hunting at night, on a web over the vegetation. **B**–**D**: *Diapontia uruguayensis* Keyserling: **B** immature from P.N. Pre-Delta, Entre Ríos, Argentina on a web on the grass; **C** immature from P.N. El Palmar, Entre Ríos, Argentina on a web on the mud; **D** male and female during copula.

Fig. 12. Live specimens. **A**: female of *Diapontia anfibia* (Zapfe-Mann) **comb.n.** (MACN-Ar 34761). **B**–**C**: female of *Diapontia niveovittata* Mello-Leitão with eggsac (MACN-Ar 32213).

Distribution. Chile and southwestern Argentina (Fig. 20A).

Natural history. Adults and immatures of this species live on the shoreline vegetation of lakes and rivers where they spin a small retreat; some specimens were collected under rocks. Adult males and females were collected throughout the year; there are only two records of eggsacs, in July and November.

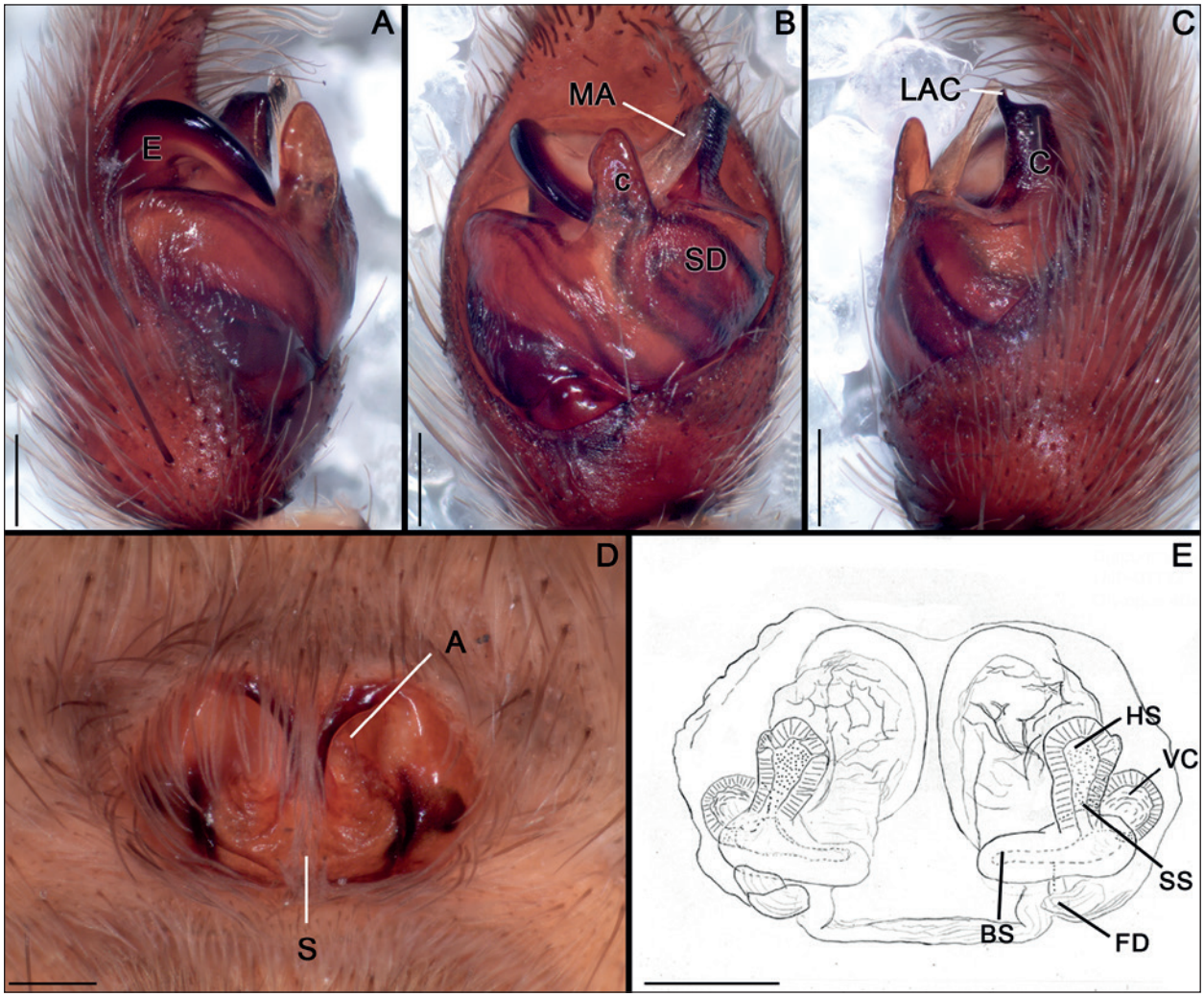

Fig. 13. *Diapontia securifera* (Tullgren) **comb.n.**, genitalia. **A**–**C**: Male from Parinacota, Chile (AMNH), palp: **A** prolateral; **B** ventral; **C** retrolateral. **D**,**E**: Female from Parinacota, Chile (AMNH): **D** epigyne ventral; **E** vulva. — ***Abbreviations***: A, atrium; BS, base of the spermatheca; C, conductor; c, ventral projection of tegulum; E, embolus; FD, fertilization ducts; HS, head of spermatheca; LAC, lateral apophysis of conductor; MA, median apophysis; S, septum; SD, sperm duct; SS, stalk of spermatheca; VC, vulval chamber. — ***Scale bars***: 0.20 mm.

3.3.5. *Diapontia securifera* (Tullgren, 1905), comb.n.

Figs. 5G,H, 6C, 13, 16A,B,G,H, 20B

Lycosa securifera Tullgren, 1905: 66, pl. 8, f. 32 (Dj).
Isohogna securifera: Roewer 1955: 262.
Porrimosa securifera: Capocasale 1982: 154.
Orinocosa securifera: Santos & Brescovit 2001: 81.

Remarks. Chamberlin (1916) cited two females from Peru, Cuzco, but upon re-examination, those specimens belong to *D. chamberlini*, a new species described below.

Differential diagnosis. Males of *Diapontia securifera* resemble those of *D. calama* and *D. songotal* by the enlarged and digitiform apophysis c (Figs. 13B, 14B, 15B) and females by the deep atria (Figs. 13D, 14D, 15D); males can be differentiated by the apical part of the conductor, with a straight end (Fig. 13C, C). Females are very hard to distinguish, but can be separated by the rectangular shape of the posterior part of the septum and by the borders of the median part of the septum having only the borders sclerotized (Fig. 13D) instead of all the anterior part of the septum as in on *D. calama* (Fig. 14D).

Description. ***Male from Chile***, ***Concepción***, ***Río Anadalién*** **(*AMNH*)**: Carapace brown with pale submarginal bands (Fig. 16B). Sternum, labium and endites dark brown (Fig. 16H). Chelicerae dark brown. Dorsum of abdomen brown with two broad parallel longitudinal white bands (Fig. 16B), venter brown with two central paler bands (Fig. 16H). Legs setose, light yellow-brown with darker areas.

Pedipalp as in Fig. 13A–C. Subtegulum small, located medially on the resting bulb. Tegulum large with a well-developed conductor, fused apically with the lateral apophysis (Fig. 13C). Apophysis c finger-like (Fig. 13B, c). Median apophysis laminar and obliquely oriented (Fig. 13B, MA); sperm duct with an S-shaped trajectory

in retroventral view (Fig. 13B, SD); embolic division without apophysis; embolus with pars pendula.

Leg formula 4123. Spination pattern: femora **I p** 0-0-0-d2 **d** 1-1-1 **r** 0-1-0-1, **II p** 0-1-0-1 **d** 1-1-1 **r** 0-1-0-1, **III p** 0-1-0-1 **d** 1-1-1 **r** 0-1-0-1, **IV p** 0-1-0-1 **d** 1-0-1-1 **r** 0-0-0-1; patellae **II r** 1, **III p** 1 **r** 1, **IV p** 1 **r** 1; tibiae **I p** d1-d1 **r** d1-d1 **v** 2-2-2ap, **II p** d1-d1 **r** d1-d1 **v** 2-2-2ap, **III p** d1-d1 **d** 1-1 **r** d1-d1 **v** 2-2-2ap, **IV p** d1-d1 **d** 1-1 **r** d1-d1 **v** 2-2-2ap; metatarsi **I p** 1-1ap **r** 1-1ap **v** 2-2-3ap, **II p** 1-1-1ap **r** 1-1-1ap **v** 2-2-3ap, **III p** 1-1-1ap **r** 1-1-1ap **v** 2-2-3ap, **IV p** 1-1-1ap **r** 1-1-1ap **v** 2-2-3ap.

Female from Chile, ***Concepción***, ***Río Anadalién*** **(*AMNH*)**: Colour in ethanol as in male but dark, submarginal bands of the carapace and parallel bands of abdomen indistinct (Fig. 16A,G).

Epigyne as in Fig. 13D with two deep atria divided by the anterior part of the septum, posterior part of the septum broad and square (Fig. 13D, S). Vulva as in Fig. 13E, base of the spermatheca enlarged centrally (Fig. 13E, BS), head of spermathecae (Fig. 13E, HS) of variable shape and short stalk, vulval chambers rounded (Fig. 13E, VC).

Leg formula 4123. Spination pattern: femora **I p** 0-0-d2 **d** 1-1-1, **II p** 0-1-0-1 **d** 1-1-1 **r** 0-1-0-1, **III p** 0-1-0-1 **d** 1-1-1 **r** 0-1-0-1, **IV p** 0-1-0-1 **d** 1-0-1-1 **r** 0-0-0-1; patellae **II r** 1, **III p** 1 **r** 1, **IV p** 1 **r** 1; tibiae **I v** p1-0-2ap, **II v** 2-2ap, **III p** d1-d1 **d** 0-1 **r** d1-d1 **v** p1-p1-2ap, **IV p** d1-d1 **d** 0-1 **r** d1-d1 **v** p1-2-2ap; metatarsi **I v** 2-2-3ap, **II p** 1-1ap **r** 0-1ap **v** 2-2-3ap, **III p** 1-1-1ap **r** 1-1-1ap **v** 2-2-3ap, **IV p** 1-1-1ap **r** 1-1-1ap **v** 2-2-3ap.

Measurements: Female, AMNH (male, AMNH): TL 7.45 (8.65), PL 3.80 (4.47), PW 2.80 (3.20), PH 1.33 (1.40), AL 3.40 (3.87). Eyes: AME 0.13 (0.18), ALE 0.12 (0.15), PME 0.25 (0.32), PLE 0.23 (0.20). Row of eyes: AER 0.83 (0.90), PMER 0.75 (0.83), PLER 1.12 (1.25). Sternum (length/width) 1.80/1.53 (2.00/1.80). Labium (length/width) 0.55/0.60 (0.58/0.67). Legs: length of segments (femur + patella/tibia + metatarsus + tarsus = total length): **I** 2.40 + 3.00 + 1.80 + 1.20 = 8.40, **II** 2.33 + 2.87 + 1.73 + 1.20 = 8.13, **III** 2.27 + 2.40 + 1.73 + 1.20 = 7.60, **IV** 2.80 + 3.40 + 2.67 + 1.60 = 10.47 (**I** 3.33 + 3.93 + 2.67 + 1.67 = 11.6, **II** 3.13 + 3.73 + 2.53 + 1.67 = 11.06, **III** 2.93 + 3.40 + 2.53 + 1.53 = 10.39, **IV** 4.27 + 4.40 + 3.40 + 2.00 = 14.07).

Variation: Female (male) (range, mean ± s.d.): TL 7.45 – 12.90, 10.71 ± 2.18; CL 3.80 – 6.33, 5.20 ± 1.00; CW 2.80 – 4.67, 3.89 ± 0.77; n = 6 (TL 8.65 – 10.37, 9.51 ± 1.22; CL 3.33 – 4.47, 3.90 ± 0.81; CW 2.53 – 3.20, 2.86 ± 0.47; n = 2). Some females have 0-r1-2ap on the ventral tibia I (MACN-Ar 23954).

Type material. HOLOTYPE of *D. securifera* ♀ 'ARGENTINA, Moreno puna de Jujuy' (NHAM).

Other material examined. See Electronic Supplement File 1.

Distribution. Northern Chile (Parinacota) and northwestern Argentina (Jujuy) (Fig. 20B).

Natural history. Some specimens were collected under rocks. A female with spiderlings were collected in January at Salar de Jama (at 4200 m a.s.l).

3.3.6. *Diapontia calama* sp.n.

Figs. 14, 16C,D,I,J, 20B

Differential diagnosis. Males of *Diapontia calama* resemble those of *D. songotal* and *D. securifera* by the enlarged and digitiform apophysis c (Figs. 13B, 14B, 15B) and females by the deep atria (Fig. 13D, 14D, 15D); males can be differentiated by the gently curved apical part of the conductor (Fig. 14C, C) and females by having a setose triangular area on the posterior part of the epigynal septum (Fig. 14D, S).

Description. ***Male*** **(*holotype*)**: Carapace brown, pale submarginal bands almost indistinct (Fig. 16D). Sternum, labium and endites dark brown (Fig. 16J). Chelicerae dark brown. Dorsum of abdomen brown with two parallel longitudinal pale bands (Fig. 16D), venter light yellow-brown (Fig. 16J). Legs with femur and patella light yellow-brown, tibia, metatarsus and tarsus brown.

Pedipalp as in Fig. 14A – C. Subtegulum small, located medially in the resting bulb. Tegulum large with a well-developed conductor, fused apically with the lateral apophysis (Fig. 14C). Apophysis c finger-like (Fig. 14B, c). Median apophysis laminar and obliquely oriented (Fig. 14B, MA); sperm duct with an S-shape starting in the retroapical part of the tegulum and ending ventrally (Fig. 14B, SD); embolic division without apophysis; embolus with pars pendula.

Leg formula 412 (Leg III missing). Spination pattern: femora **I p** 0-0-0-d2 **d** 1-1-1 **r** 0-1-0-1, **II p** 0-1-0-1 **d** 1-1-1 **r** 0-1-0-1, **IV p** 0-1-0-1 **d** 1-0-1-1 **r** 0-0-0-1; patellae **I p** 1 **r** 1, **II p** 1 **r** 1, **III - IV p** 1 **r** 1; tibiae **I p** d1-d1 **v** 2-2-2ap **r** d1-d1, **II p** d1-d1 **v** 2-2-2ap, **IV p** d1-d1 **d** 1-1 **r** d1-d1 **v** 2-2-2ap; metatarsi **I p** 1-1ap **v** 2-2-3ap **r** 1-1ap, **II p** 1-1-1ap **v** 2-2-3ap **r** 1-1-1ap, **IV p** 1-1-1ap **r** 1-1-1ap **v** 2-2-3ap.

Female from Chile, ***Calama*** **(*MNHN 903*)**: Colour in ethanol as in male, but less contrasting (Fig. 16C,I).

Epigyne as in Fig. 14B with the atria deep and separated by a narrow septum with a sclerotised border, posterior part of the septum enlarged, triangular in shape (Fig. 14D, S). Vulva as in Fig. 14E, head of spermathecae round (Fig. 14E, HS), sligtly wider than the short stalk, vulval chambers round (Fig. 14E, VC).

Leg formula 4132. Spination pattern: femora **I p** 0-0-d2 **d** 1-1-1 **r** 0-1-0-1, **II p** 0-1-0-1 **d** 1-1-1 **r** 0-1-0-1, **III p** 0-1-0-1 **d** 1-1-1 **r** 0-1-0-1, **IV p** 0-1-0-1 **d** 1-0-1-1 **r** 0-0-0-1; patellae **III r** 1, **IV p** 1 **r** 1; tibiae **I v** 2-2ap **r** d1-d1, **II p** d1-d1 **v** 2-2ap, **III p** d1-d1 **d** 1-1 **r** d1-d1 **v** p1-2-2ap, **IV p** d1-d1 **d** 1-1 **r** d1-d1 **v** p1-2-2ap; metatarsi **I p v** 2-2-3ap **II p** 1-0 **v** 2-2-3ap **r** 1-0, **III p** 1-1-1ap **r** 1-1-1ap **v** 2-2-3ap, **IV p** 1-1-1ap **r** 1-1-1ap **v** 2-2-3ap. Ventral spines of tibia I and II small.

Measurements: Female. MNHN 903 (male, holotype): TL 13.03 (11.04), PL 7.32 (5.67), PW 4.07 (4.07), PH 2.00 (1.87), AL 7.85 (4.67). Eyes: AME 0.20 (0.18), ALE 0.23 (0.20), PME 0.33 (0.32), PLE 0.35 (0.33). Row of eyes: AER 1.18 (1.08), PMER 1.07 (0.97), PLER 1.63 (1.47). Sternum (length/width) 2.47/2.20 (2.47/2.07). La-

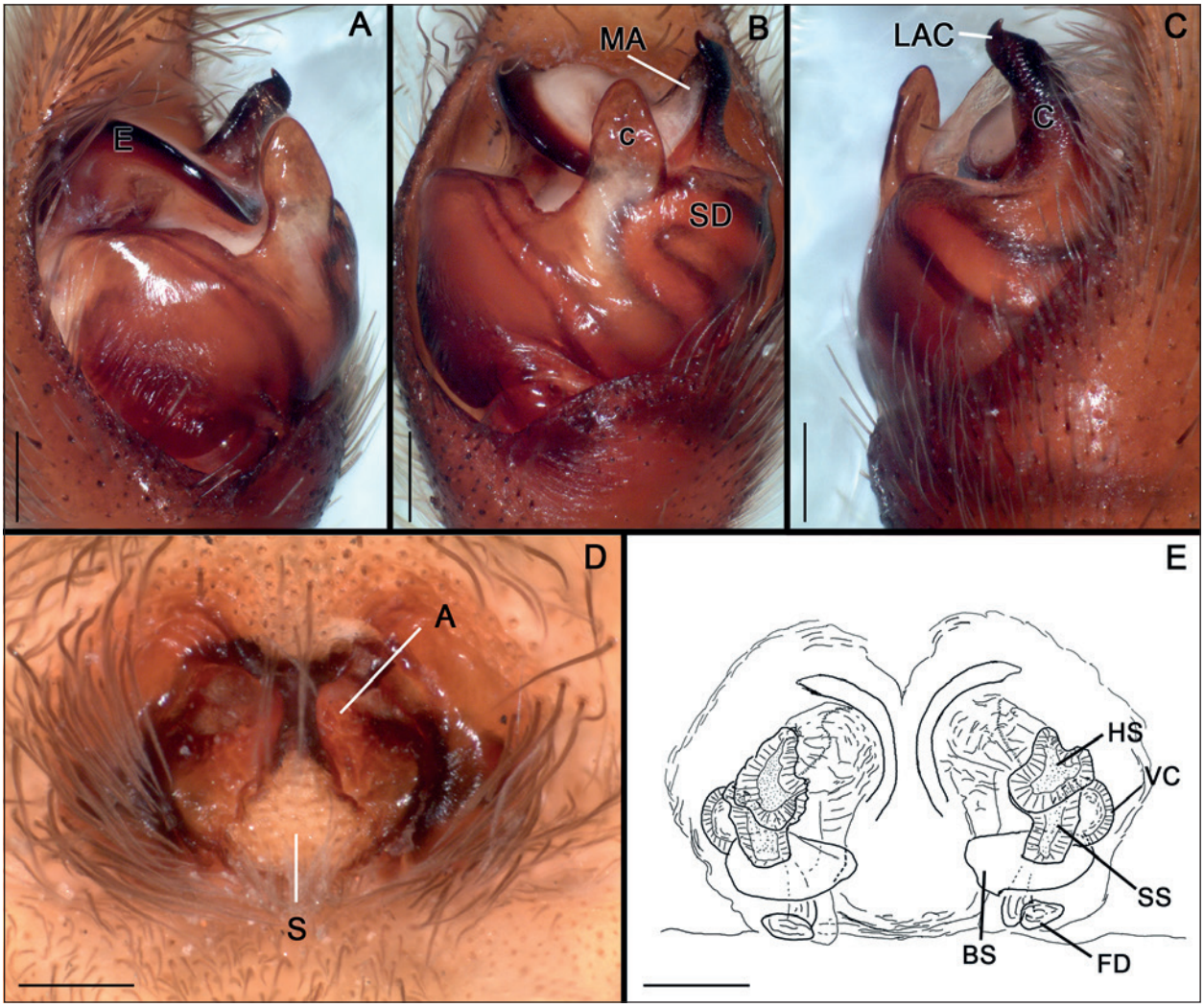

Fig. 14. *Diapontia calama* **sp.n.**, genitalia. **A**–**C**: Male from Calama, Chile (holotype), palp: **A** prolateral; **B** ventral; **C** retrolateral. **D**–**E**: Female from Calama, Chile (MHN 903): **D** epigyne ventral; **E** vulva. — ***Abbreviations***: A, atrium; BS, base of the spermatheca; C, conductor; c, ventral projection of tegulum; E, embolus; FD, fertilization ducts; HS, head of spermatheca; LAC, lateral apophysis of conductor; MA, median apophysis; S, septum; SD, sperm duct; SS, stalk of spermatheca; VC, vulval chamber. — ***Scale bars***: 0.20 mm.

bium (length/width) 0.92/0.90 (0.75/0.77). Legs: length of segments (femur + patella/tibia + metatarsus + tarsus = total length): **I** 3.47 + 4.33 + 2.67 + 1.73 = 12.2, **II** 3.33 + 4.33 + 2.47 + 1.73 = 11.86, **III** 3.33 + 3.93 + 2.73 + 1.73 = 11.72, **IV** 4.07 + 5.13 + 4.13 + 2.13 = 15.46 (**I** 3.87 + 5.47 + 3.60 + 2.13 = 15.07, **II** 3.73 + 5.27 + 3.67 + 2.00 = 14.67, **IV** 4.67 + 5.60 + 5.33 + 2.33 = 17.93).

Variation: Female (male) (range, mean ± s.d.): TL 9.31–14.76 12.37±1.42; CL 5.07–7.71, 6.33±0.73; CW 3.93–5.53, 4.73±0.45; n = 10 (TL 11.04–11.44, 11.24±0.28; CL 5.67–6.33, 6.00±0.47; CW 4.047–4.06, 4.33±0.37; n = 2).

Etymology. The specific epithet is a noun in apposition referring to the type locality.

Type material. HOLOTYPE ♂ and ♂ PARATYPE 'Calama, i.1983, Arriaga coll' | 'Diapontia sp. Éder Álvares det.' | 'MNHN 680'. PARATYPE 10 ♀ two eggsacs, 'La Cascada, 10.i.1984, Arriaga coll' | 'MNHN 904'.

Other material examined. See Electronic Supplement File 1.

Distribution. Northern of Chile (Calama Province) and an uncertain locality in Bolivia ("El Cumbre") (Fig. 20B).

3.3.7. *Diapontia songotal* sp.n.

Figs. 15, 16E,F,K,L, 20B

Differential diagnosis. Males of *D. songotal* resemble those of *D. calama* and *D. securifera* by the enlarged and digitiform apophysis c (Figs. 13B, 14B, 15B) and females by the deep atria (Figs. 13D, 14D, 15D); males can be differentiated by the curved apical part of the conductor (Fig. 15C, C). Females can be distinguished by the lateral lobes reach the median part of septum (Fig. 15D, LL).

Description. ***Male* (*holotype*)**: Carapace reddish-brown with pale submarginal bands (Fig. 16F). Sternum, labium and endites dark brown (Fig. 16L). Chelicerae dark brown. Dorsum of abdomen brown with two parallel longitudinal pale bands lined by dark brown (Fig. 16F),

Fig. 15. *Diapontia songotal* **sp.n.**, genitalia. **A**–**C**: Male holotype, palp: **A** prolateral; **B** ventral; **C** retrolateral. **D**: Epigyne ventral (female paratype). **E** vulva (female paratype). **F**: Epigyne ventral (female from Chacaltaya). **G**: Epigyne ventral (female from Songotal). **H**: Epigyne ventral (female from Chacaltaya). **I**: Epigyne ventral (female from Cuticucho). — ***Abbreviations***: A, atrium; BS, base of the spermatheca; C, conductor; c, ventral projection of tegulum; E, embolus; FD, fertilization ducts; HS, head of spermatheca; LAC, lateral apophysis of conductor; LL, lateral lobes of epigyne; MA, median apophysis; S, septum; SD, sperm duct; SS, stalk of spermatheca; VC, vulval chamber. — ***Scale bars***: 0.20 mm.

venter light yellow-brown (Fig. 16L). Legs light yellow-brown with dark areas.

Pedipalp as in Fig. 15A–C. Subtegulum small, located mesally in the resting bulb (Fig. 15B). Tegulum large, with a well-developed conductor, fused apically with the lateral apophysis of the conductor (Fig. 15B). Apophysis c strongly developed, finger-like (Fig. 15B). Median apophysis laminar and obliquely oriented (Fig. 15B); sperm duct with a S-shape curve starting on the retroapical part of the tegulum and ending ventrally (Fig. 15B,C, SD); embolic division without apophysis; embolus with a pars pendula well-developed (Fig. 15B).

Leg formula 4132. Spination pattern: femora **I p** 0-0-d2 **d** 1-1-1 **r** 0-1-1, **II p** 0-0-1 **d** 1-1-0 **r** 0-2-1, **III p** d1-d1 **d** 1-1-1 **r** d1-d1, **IV p** d1-d1 **d** 1-1-1 **r** 0-d1; patellae **II p** 1 **r** 1, **III p** 1 **r** 1, **IV p** 1 **r** 1; tibiae **I p** 1-1 **v** 2-2-2ap **r** 1-1, **II p** d1-d1 **v** 2-2-2ap, **III p** 1-1 **d** 1-1-1 **r** 1-1 **v** 2-2-2ap, **IV p** 1-1 **d** 1-1-0 **r** 1-1 **v** p1-2-2ap; metatarsi **I p** 0-1-1ap **r** 0-1-1ap **v** 2-2-1ap, **II p** 0-1-2ap **r** 0-1-2ap **v** 2-2-1ap, **III p** 1-1-2ap **r** 1-1-2ap **v** 2-2-1ap, **IV p** 1-1-2ap **r** 1-1-2ap **v** 2-2-1ap.

***Female* (*paratype*)**: Colour in ethanol as in male but with less contrasting, the submarginal bands of the carapace lost most of the pale setae and the abdomen lacks the dorsal bands (Fig. 16E,K).

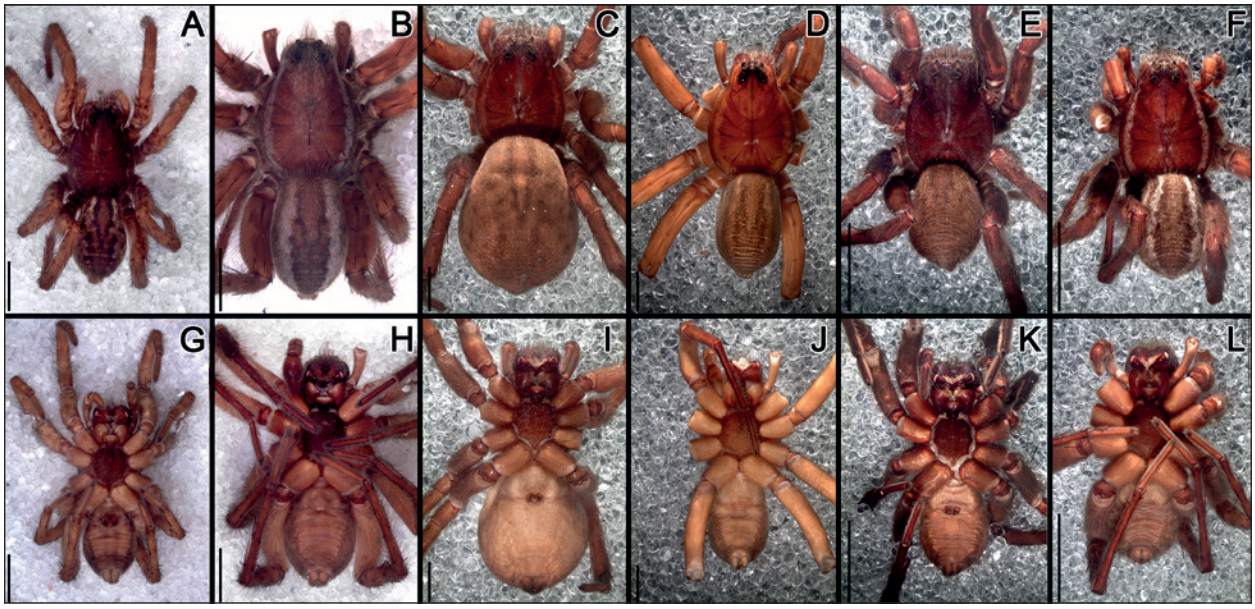

Fig. 16. Habitus, **A**–**F** dorsal, **G**–**L** ventral. **A**,**B**,**G**,**H**: *Diapontia securifera* (Tullgren) **comb.n.**: **A**,**G** female; **B**,**H** male. **C**,**D**,**I**,**J**: *Diapontia calama* **sp.n.**: **C**,**I** female; **D**,**J** male. **E**,**F**,**K**,**L**: *Diapontia songotal* **sp.n.**: **E**,**K** female; **F**,**L** male. — ***Scale bars***: A–D,G–H 2.00 mm; E–F,K–L 5.00 mm.

Epigyne as in Fig. 15D, septum with an anchor shape (Fig. 15D), anterior part of septum limited by two deep atria, lateral lobes reach the septum in the middle part (Fig. 15D, LL). Vulva as in Fig. 15E with the base of the spermatheca broader centrally, head of spermathecae (Fig. 15E, HS) slightly larger than the short stalk, vulval chambers rounded (Fig. 15E, VC).

Leg formula 4132. Spination pattern: femora **I p** 0-0-d2 **d** 0-1-1, **II p** d1-d1 **d** 1-1-1 **r** d1-d1, **III p** d1-d1 **d** 1-1-1 **r** d1-d1, **IV p** 0-d1 **d** 1-1-1 **r** 0-d1; patellae **III p** 1 **r** 1, **IV p** 1 **r** 1; tibiae **I v** 2-2-2ap, **II p** 0-d1 **v** 2ap, **III p** d1-d1 **r** d1-d1 **v** p1-p1-2ap, **IV p** d1-d1 **d** 0-1 **r** d1-d1 **v** p1-2-2ap; metatarsi **I p** 0-0-1ap **r** 0-0-1ap **v** 2-2-1ap, **II p** 0-1-1ap **r** 0-1-2ap **v** 2-2-1ap, **III p** 1-1-2ap **r** 1-1-2ap **v** 2-2-1ap, **IV p** 1-1-2ap **r** 1-1-2ap **v** 2-2-1ap.

Measurements: Female paratype (male holotype): TL 12.5 (12.64), PL 4.93 (6.67), PW 4.27 (5.40), PH 1.73 (1.87), AL 6.67 (6.47). Eyes: AME 0.17 (0.22), ALE 0.17 (0.20), PME 0.32 (0.43), PLE 0.25 (0.35). Row of eyes: AER 1.17 (1.35), PMER 0.97 (1.20), PLER 1.52 (1.80). Sternum (length/width) 2.80/2.07 (3.47/2.47). Labium (length/width) 1.00/0.90 (1.28/1.07). Legs: length of segments (femur + patella/tibia + metatarsus + tarsus = total length): **I** 4.12 + 5.05 + 2.93 + 2.00 = 14.10, **II** 3.99 + 4.66 + 2.79 + 1.73 = 13.17, **III** 3.99 + 4.52 + 3.33 + 1.86 = 13.70, **IV** 4.66 + 5.85 + 4.52 + 2.66 = 17.69 (**I** 5.59 + 7.85 + 5.32 + 2.66 = 21.42, **II** 5.45 + 6.52 + 4.92 + 2.66 = 19.55, **III** 5.45 + 6.52 + 5.32 + 2.53 = 19.82, **IV** 6.52 + 8.38 + 7.05 + 3.46 = 25.41).

Variation: Female (male) (range, mean ± s.d.): TL 11.04–18.36, 12.90 ± 0.1.96; CL 3.33–6.67, 5.51 ± 0.89; CW 4.27–5.60, 4.85 ± 0.68; n = 10 (TL 9.58–12.64, 11.11 ± 2.16; CL 4.67–6.67, 5.67 ± 1.41; CW 3.67–5.40, 4.53 ± 1.22; n = 3). Variations on the shape of the median septum are illustrated in Fig. 15F–I.

Etymology. The specific epithet is a noun in apposition referring to the type locality.

Type material. HOLOTYPE ♂ and ♂ ♀ PARATYPE 'AMNH Bolivia: Chacaltaya, alt. 4700 m, 24–25.iv.1954, in a small field under rock, Forster & Schindler.' ♀ PARATYPE 'AMNH Bolivia, Songotal, 1.xii.1953, Forster & Schindler, under rock'

Other material examined. See Electronic Supplement File 1.

Distribution. West central Bolivia (La Paz province) (Fig. 20B).

Natural history. Adult males were recorded in January, March and December, and adult females from November to March; there are only two records of eggsacs from February and November. Some specimens were collected under stones (data from label).

3.3.8. *Diapontia arapensis* (Strand, 1908) comb.n.

Tarentula arapensis Strand 1908: 245.
Lycosa arapensis: Petrunkevitch 1911: 555; Bonnet 1957: 2633.
Mimohogna arapensis: Roewer 1955: 279.
Lycosa arapensis: Fuhn & Niculescu-Burlacu 1971: 193.
Hippasella arapensis: Brescovit & Álvares 2011: 57.

Remark. The S-shaped trajectory of the sperm duct (Álvares & Brescovit 2007: figs. 17, 18) on the male bulb and the short stalk of the spermatheca (Álvares & Brescovit 2007: fig. 21) of females justifies the transfer of the specimen from *Hippasella* to *Diapontia*.

Description. See Brescovit & Álvares (2011).

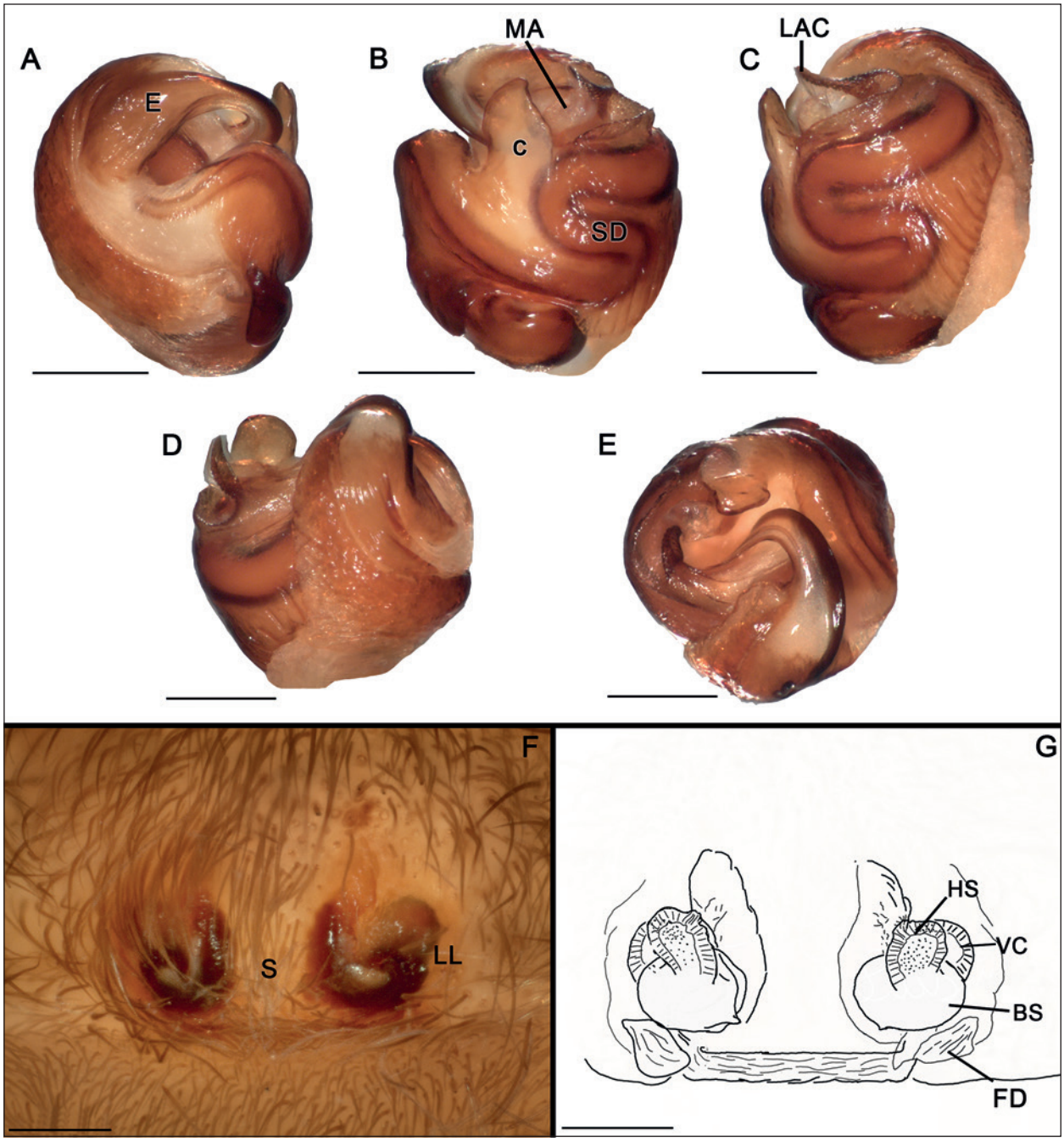

Fig. 17. *Diapontia chamberlini* **sp.n.**, genitalia. **A**–**E**: Male from Andahuaylas, (holotype), bulb: **A** prolateral; **B** ventral; **C** retrolateral; **D** dorsal; **E** apical. **F**,**G**: Female from Andahuaylas, Perú (paratype): **F** epigyne ventral; **G** vulva. — ***Abbreviations***: A, atrium; BS, base of the spermatheca; C, conductor; c, ventral projection of tegulum; E, embolus; FD, fertilization ducts; HS, head of spermatheca; LAC, lateral apophysis of conductor; LL, lateral lobes of epigyne; MA, median apophysis; S, septum; SD, sperm duct; VC, vulval chamber. — ***Scale bars***: 0.20 mm.

Differential diagnosis. Males of *Diapontia arapensis* resemble those of *D. chamberlini* and *D. oxapampa* by the thin embolus and poorly developed apophysis c (Brescovit & Álvares 2011: fig. 17) and females by the broad and setose septum (Brescovit & Álvares 2011: fig. 19); males can be differentiated by the strong develop of the LAC and C (Brescovit & Álvares 2011: fig. 17); females by the long anchor-shaped of the septum (Brescovit & Álvares 2011: fig. 19).

Material examined. See Electronic Supplement File 1.

3.3.9. *Diapontia chamberlini* sp.n.

Figs. 17, 19A,B,E,F, 20C

Lycosa securifera: Chamberlin 1916: 282. Misidentification.

Differential diagnosis. Males of *D. chamberlini* resemble those of *D. arapensis* and *D. oxapampa* by the thin embolus and poor developed apophysis c (Brescovit & Álvares 2011: fig. 17) and females by the broad and setose septum (Brescovit & Álvares 2011: fig. 19); by the elongated apophysis c (Fig. 17B); females have a broad

septum with a sclerotised border in the posterior part of the epigyne (Fig. 17F).

Description. ***Male* (*holotype*)**: Carapace brown with pale submarginal bands (Fig. 19A). Sternum, labium and endites brown (Fig. 19E). Chelicerae brown. Dorsum of abdomen brown with two parallel longitudinal pale bands (Fig. 19A), venter light yellow-brown (Fig. 19E). Legs light yellow-brown with dark areas.

Pedipalp as in Fig. 17A–E. Subtegulum small, located mesally in the resting bulb (Fig. 17B). Tegulum large with a small conductor, fused with the lateral apophysis (Fig. 17C, LAC), apophysis c enlarged (Fig. 17B, c). Median apophysis laminar and longitudinally directed (Fig. 17B, MA); sperm duct with an S-shaped trajectory in retroventral view (Fig. 17B, SD); embolic division without apophysis (Fig. 17E); embolus with a pars pendula well-developed (Fig. 17E).

Leg formula 4123. Spination pattern: femora **I p** 0-0-d2 **d** 1-1, **r** d1-d1, **II p** d1-d1 **d** 1-1-1 **r** d1-d1, **III p** d1-d1 **d** 1-1-1 **r** d1-d1, **IV p** 1-d1 **d** 1-1-1 **r** 0-d1; patellae **II p** 1 **r** 1, **III p** 1 **r** 1, **IV p** 1 **r** 1; tibiae **I p** 1-1 **v** 2-2-2ap **r** 1-1, **II p** 1-d1 **v** p1-2-2ap **r** 1-1, **III p** d1-d1 **d** 1 **r** d1-d1 **v** 2-2-2ap, **IV p** d1-d1 **d** 1-1 **r** d1-d1 **v** 2-2-2ap; metatarsi **I p** 1-1ap **r** 1-1ap **v** 2-2-1ap, **II p** 0-1-2ap **r** 0-1-2ap **v** 2-2-1ap, **III p** 1-1-2ap **r** 1-1-2ap **v** 2-2-1ap, **IV p** 1-1-2ap **r** 1-1-2ap **v** 2-2-1ap.

***Female* (*paratype*)**: Colour in ethanol as in male but less contrasting, the submarginal bands of the carapace very indistinct, and the abdomen lacks the dorsal pale bands (Fig. 19B,F).

Epigyne as in Fig. 17F, septum broad and setose, lateral lobes slightly sclerotised (Fig. 17F, LL). Vulva (Fig. 17G), stalk of the spermatheca short, head of spermathecae round (Fig. 17G, HS), vulval chamber rounded (Fig. 17G, VC).

Leg formula 4123. Spination pattern: femora **I p** 0-0-d2 **d** 1-1, **II p** d1-d1 **d** 1-1-1 **r** 0-d1, **III p** d1-d1 **d** 1-1-1 **r** d1-d1, **IV p** d1-d1 **d** 1-1-1 **r** 0-d1; patellae **III p** 1 **r** 1, **IV p** 1 **r** 1; tibiae **I p** 1-d1 **v** 2-0-2ap, **II p** d1-1 **v** r1-0-2ap, **III p** d1-d1 **d** 1 **r** d1-d1 **v** p1-p1-2ap, **IV p** d1-d1 **d** 0-1 **r** d1-d1 **v** p1-2-2ap; metatarsi **I p** 0-1ap **r** 0-1ap **v** 2-2-1ap, **II p** 0-1ap **r** 0-1ap **v** 2-2-1ap, **III p** 1-1-2ap **r** 1-1-2ap **v** 2-2-1ap, **IV p** 1-1-2ap **r** 1-1-2ap **v** 2-2-1ap.

Measurements: Female paratype (male holotype): TL 14.23 (7.58), PL 6.00 (3.80), PW 4.73 (3.00), PH 2.27 (1.40), AL 7.98 (3.53). Eyes: AME 0.18 (0.13), ALE 0.18 (0.13), PME 0.35 (0.25), PLE 0.33 (0.23). Row of eyes: AER 1.32 (0.87), PMER 1.08 (0.80), PLER 1.67 (1.15). Sternum (length/width) 2.87/2.33 (2.00/1.67). Labium (length/width) 1.00/0.97 (0.58/0.60). Legs: length of segments (femur + patella/tibia + metatarsus + tarsus = total length): **I** 4.33 + 4.73 + 3.07 + 2.00 = 14.13, **II** 4.13 + 4.73 + 2.93 + 1.67 = 13.46, **III** 4.00 + 4.40 + 2.87 + 1.67 = 12.94, **IV** 4.87 + 5.67 + 4.40 + 2.33 = 17.27 (**I** 3.00 + 3.93 + 2.67 + 1.67 = 11.27, **II** 3.00 + 3.67 + 2.53 + 1.60 = 10.80, **III** 2.73 + 3.20 + 2.53 + 1.60 = 10.06, **IV** 3.53 + 4.27 + 3.87 + 1.87 = 13.54).

Variation: Female (male) (range, mean ± s.d.): TL 9.58–14.23, 11.62 ± 1.68; CL 4.67–6.00, 5.35 ± 0.45; CW 3.07–4.87, 4.22 ± 0.57; n = 8 (TL 7.58–10.91, 9.27 ± 1.66; CL 3.80–5.00, 4.60 ± 0.69; CW 3.00–4.33, 3.78 ± 0.69; n = 3).

Etymology. The specific name is a patronym in honor of the late Dr. R.V. Chamberlin, in recognition of his pioneering work on lycosid genitalia and taxonomy.

Type material. HOLOTYPE ♂ '43 km. N. Andahuaylas PERU III-7-51 3500 m Ross & Michelbacher' | 'CASENT 9047116' and 2 ♂ 5 ♀ 3 immatures PARATYPES '43 km. N. Andahuaylas PERU III-7-51 3500 m, Ross & Michelbacher' | 'CASENT 9039903'

Other material examined. See Electronic Supplement File 1.

Distribution. Central and southern Peru (Fig. 20C).

Natural history. The only data available are from the records of Chamberlin (1911) who noted that the specimens were collected under rocks. Adult males were recorded in March and October; females in March to May, in July and October; and there is only one record of a female with eggsac in July.

3.3.10. *Diapontia oxapampa* sp.n.

Figs. 6D,H, 18, 19C,D,G,H, 20C

Differential diagnosis. Males of *Diapontia oxapampa* resemble those of *D. arapensis* and *D. chamberlini* by the thin embolus and poorly developed apophysis c (Fig. 18B) and females by the broad and setose septum (Fig. 18D); differentiated by the triangular shape of apophysis c (Fig. 18B, c); females by the triangular shape of the posterior part of the septum (Figs. 6H, 18D).

Description. ***Male* (*holotype*)**: Carapace brown with pale submarginal bands (Fig. 19C). Sternum, labium and endites brown (Fig. 19G). Chelicerae brown. Dorsum of abdomen brown with two parallel longitudinal pale bands (Fig. 19C), venter light yellow-brown (Fig. 19G). Legs light yellow-brown with dark areas.

Pedipalp as in Fig. 18A–C. Subtegulum small, located mesally, slightly displaced prolaterally on the resting bulb (Fig. 18B). Tegulum large with a small conductor, fused with the lateral apophysis (Fig. 18C, LAC). Apophysis c triangular (Fig. 18B, c). Median apophysis laminar and obliquely directed (Fig. 18B, MA); sperm duct with a S-shape starting on the retroapical part of the tegulum and finishing ventrally (Fig. 18B,C, SD); embolic division without apophysis.

Leg formula 4132. Spination pattern: femuora **I p** 0-d2 **d** 1-1-1 **r** 1-1, **II p** d1-d1 **d** 1-1-0 r d1-d1, **III p** d1-d1 **d** 1-1-1 **r** d1-d1, **IV p** d1-d1 **d** 1-1-1 **r** 0-d1; patellae **I p** 1, **II p** 1, **III p** 1 **r** 1, **IV p** 1 **r** 1; tibiae **I** p d1-d1 **v** 2-2-2ap **r** d1-d1, **II p** d1-d1 **v** 2-2-2ap **r** d1-d1, **III p** 1-1 **d** 1-1 **r** 1-1 **v** r1-2-2ap, **IV p** 1-1 **d** 1-1 **r** 1-1 **v** 2-2-2ap; metatarsi I **p** 0-1-1ap **r** 0-1-1ap **v** 2-2-1ap, **II p** 0-1-2ap **r** 0-1-2ap **v** 2-2-1ap, **III p** 1-1-2ap **r** 1-1-2ap **v** 2-2-1ap, **IV p** 1-1-2ap **r** 1-1-2ap **v** 2-2-1ap.

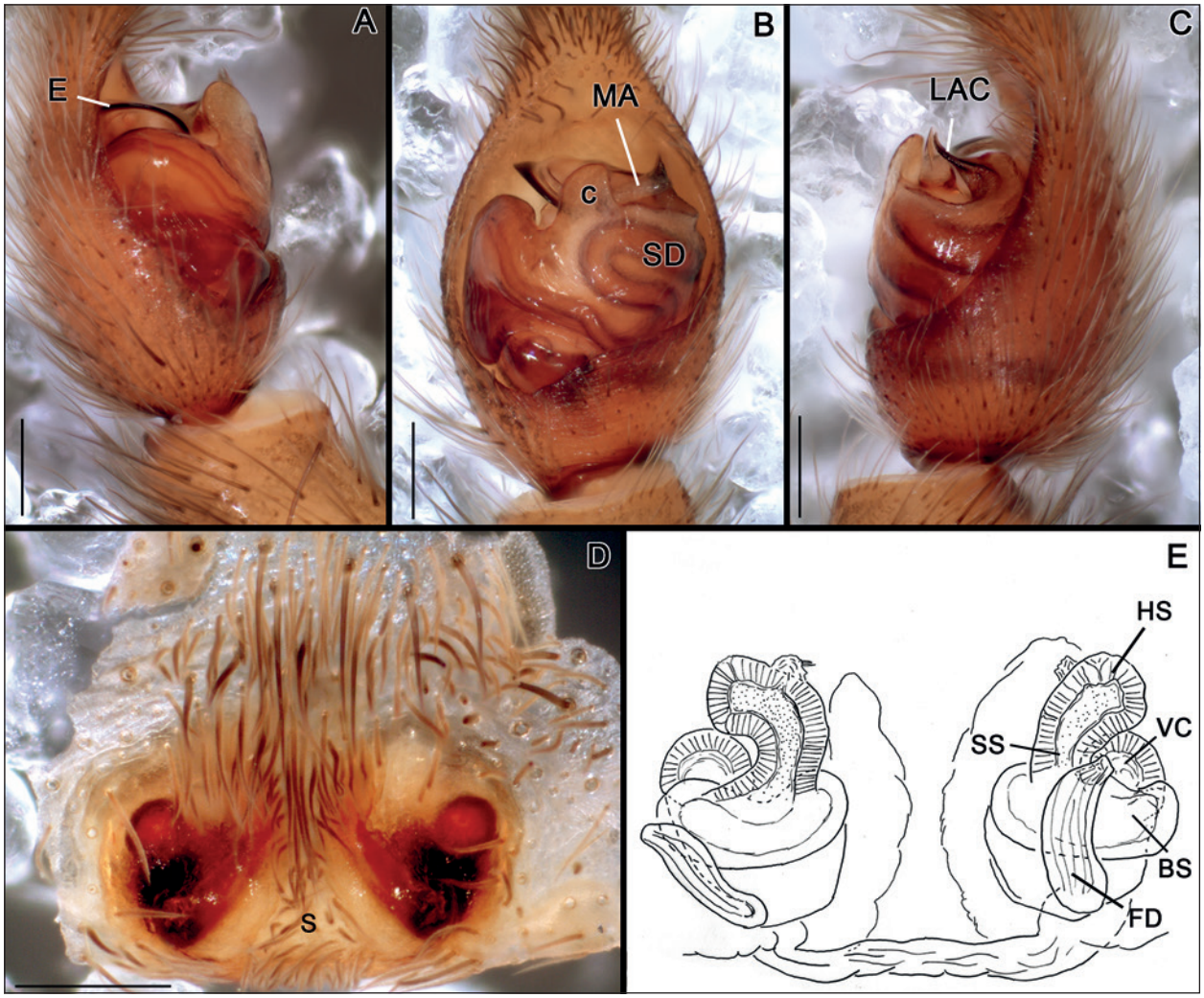

Fig. 18. *Diapontia oxapampa* **sp.n.**, genitalia. **A**–**C**: Male from Oxapampa, Perú (holotype), bulb: **A** prolateral; **B** ventral; **C** retrolateral. **D**,**E**: Female from Oxapampa, Perú (paratype). **D** epigyne ventral. **E** vulva. — ***Abbreviations***: BS, base of the spermatheca; c, ventral projection of tegulum; E, embolus; FD, fertilization ducts; HS, head of spermatheca; LAC, lateral apophysis of conductor; MA, median apophysis; S, septum; SD, sperm duct; SS, stalk of spermatheca; VC, vulval chamber. — ***Scale bars***: 0.20 mm.

***Female* (*paratype*)**: Colour in ethanol as in male, except for the abdomen, which is dorsally brown, without the clear bands (Fig. 19D,H).

Epigyne as in Fig. 18D, with the septum enlarged posteriorly, triangular in shape (Fig. 18D, S). Vulva as in Fig. 18E, head of spermathecae similar in width to the short stalk, vulval chamber round (Fig. 18E, VC).

Leg formula 4123. Spination pattern: femora **I p** 0-d2 **d** 1-1-1, **II p** d1-d1 **d** 1-1-1 r d1-d1, **III p** d1-d1 **d** 1-1-1 **r** d1-d1, **IV p** d1-d1 **d** 1-1-1 **r** 0-d1; patellae **II p** 1, **III p** 1 **r** 1, **IV p** 1 **r** 1; tibiae **I v** 2-2-2ap, **II p** d1-d1 **v** 0-r1-2ap, **III p** d1-d1 **d** 0-1 **r** d1-d1 **v** p1-2-2ap, **IV p** 1-1 **d** 0-1 **r** 1-1 **v** p1-2-2ap; metatarsi I **p** 0-0-1ap **r** 0-0-1ap **v** 2-2-1ap, **II p** 0-1-1ap **r** 0-1-1ap **v** 2-2-1ap, **III p** 1-1-2ap **r** 1-1-2ap **v** 2-2-1ap, **IV p** 1-1-2ap **r** 1-1-2ap **v** 2-2-1ap.

Measurements: Female paratype (male holotype): TL 8.25 (7.45), PL 3.80 (3.67), PW 3.07 (3.00), PH 1.47 (1.73), AL 4.00 (4.07). Eyes: AME 0.15 (0.10), ALE 0.17 (0.13), PME 0.28 (0.25), PLE 0.23 (0.27). Row of eyes: AER 0.95 (0.82), PMER 0.87 (0.77), PLER 1.25 (1.17). Sternum (length/width) 2.00/1.60 (2.00/1.47). Labium (length/width) 0.67/0.70 (0.58/0.67) Legs: length of segments (femur + patella/tibia + metatarsus + tarsus = total length): **I** 2.80 + 3.47 + 2.00 + 1.20 = 9.47, **II** 2.67 + 3.33 + 2.00 + 1.20 = 9.20, **III** 2.33 +3.07 + 2.07 + 1.20 = 8.67, **IV** 3.33 + 4.47 + 3.27 + 1.40 = 12.47 (**I** 2.93 + 3.80 + 2.47 + 1.40 = 10.60, **II** 2.80 + 3.47 + 2.47 + 1.33 = 10.07, **III** 2.67 + 3.00 + 2.47 + 2.40 = 10.54, **IV** 3.47 + 4.33 + 3.67 + 1.73 = 13.20).

Variation: Female (range, mean ± s.d.): TL 7.98 – 13.17, 9.88 ± 1.79; CL 3.80 – 5.33, 4.69 ± 0.52; CW 3.07 – 4.07, 3.53 ± 0.40; n = 7.

Etymology. The specific epithet is a noun in apposition referring to the type locality.

Type material. ♂ HOLOTYPE and 7 ♀ PARATYPES 'Peru: Pasco: Oxapampa, tanque de agua, alt. 1909 m, 10°34′50.5″S, 75°23′46.5″W, 15.i.2004, Silva, Granes & Böttger, J. MUSM-ENT 0505181'.

Other material examined. See Electronic Supplement File 1.

Distribution. Only know from the type locality in Oxapampa at northern of Peru (Fig. 20C).

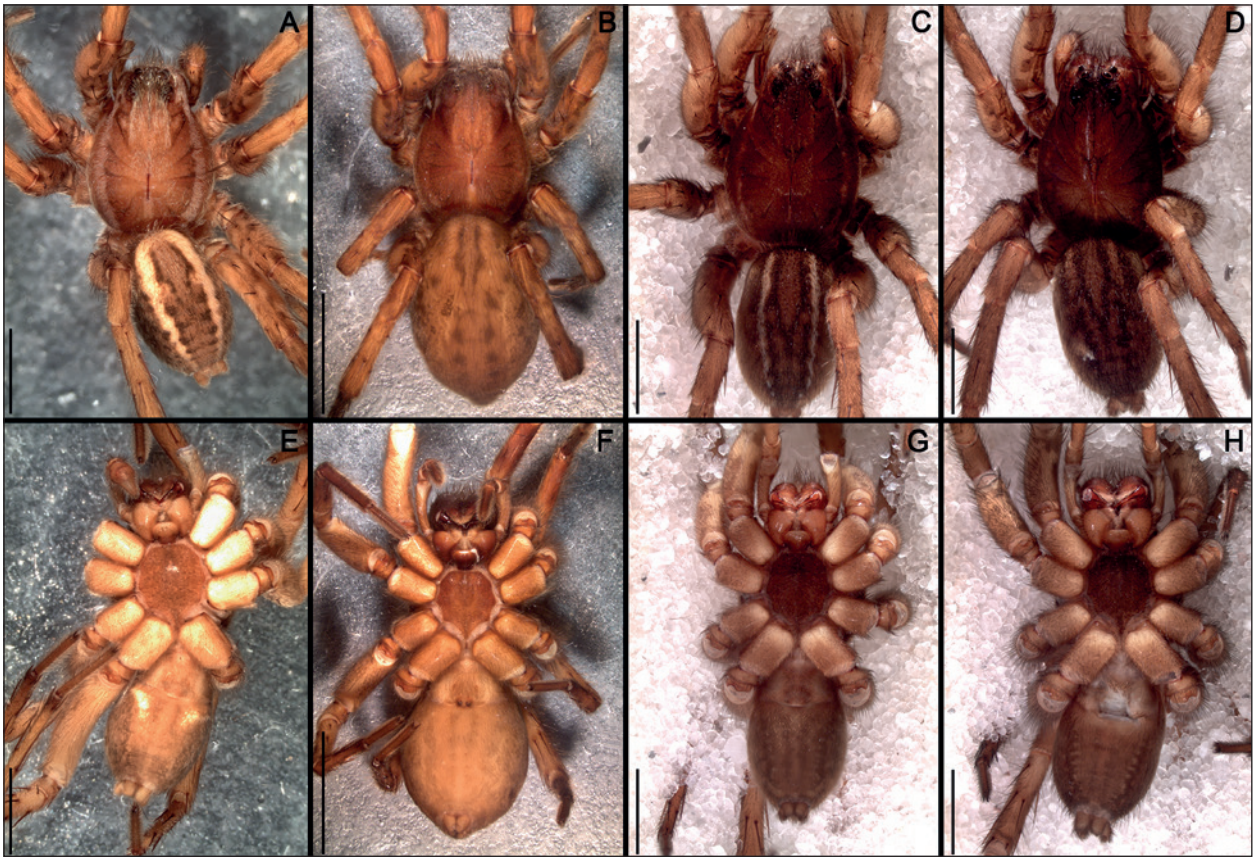

Fig. 19. Habitus, **A**–**D** dorsal, **E**–**F** ventral. **A**,**B**,**E**,**F**: *Diapontia chamberlini* **sp.n.**: **A**,**E** male; **B**,**F** female. **C**,**D**,**G**,**H**: *Diapontia oxapampa* **sp.n.**: **C**,**G** male; **G**,**H** female. — ***Scale bars***: A,C–E,G,H 2.00 mm; B,F 5.00 mm.

4. Discussion

4.1. Phylogeny of Lycosidae

Lycosidae and Trechaleidae were recovered with high posterior probability and strong bootstrap support, and the relationships between Lycosidae, Pisauridae and Trechaleidae corroborate the findings of studies based on morphological (Griswold 1993) and molecular (Wheeler et al. 2017; Albo et al. 2017) analyses, in which the Trechaleidae is the sister-group of Lycosidae (Fig. 1).

The intrafamiliar relationships of Lycosidae that were recovered in this study generally agree with the topology of the Bayesian tree obtained by Murphy et al. (2006: fig. 3) although we obtained greater support for Sosippinae and Artoriinae. The subfamily Allocosinae (*Allocosa* and *Gnatholycosa*), included here for the first time in a molecular phylogeny, were strongly supported as monophyletic, but the relationship with other lycosid subfamilies was not conclusive in our analysis. For example, the Allocosinae were recovered as sister to *Xerolycosa* (Evippinae) (Bayesian tree, with low support) or sister to Lycosinae + Pardosinae (maximum likelihood, with moderate bootstrap support; Figs. S2.5) as Dondae (1986) suggested. The subfamily Zoicinae, represented by the type genus *Zoica* Simon, 1898 was nested within Piratinae, represented by *Pirata* Sundevall, 1833 and *Piratula* Roewer, 1960, suggesting that Piratinae may be a junior synonym of Zoicinae. However, we have postponed a decision on this issue until a broader analysis, which is in progress by the first and last authors, is concluded.

4.2. Subfamily placement

Our molecular phylogenetic analyses recovered the genus *Diapontia* within Sosippinae, as suggested by Álvares & Brescovit (2007), and this was confirmed by morphological characters, including the absence of a terminal apophysis and the presence of a lateral apophysis of the conductor. The characters regarding the tegular groove and the position of resting embolus, proposed by Dondale (1986) as diagnostic for Sosippinae are, however, absent in *Diapontia* and *Hippasella* (Piacentini 2011: fig. 2). Therefore, the diagnostic characters proposed for Sosippinae must be re-evaluated – a task that is beyond the scope of the present work.

4.3. Web evolution

The internal structure of Sosippinae that was recovered in our analyses indicates a tendency toward the loss of the funnel web in the subfamily. Independent multiple

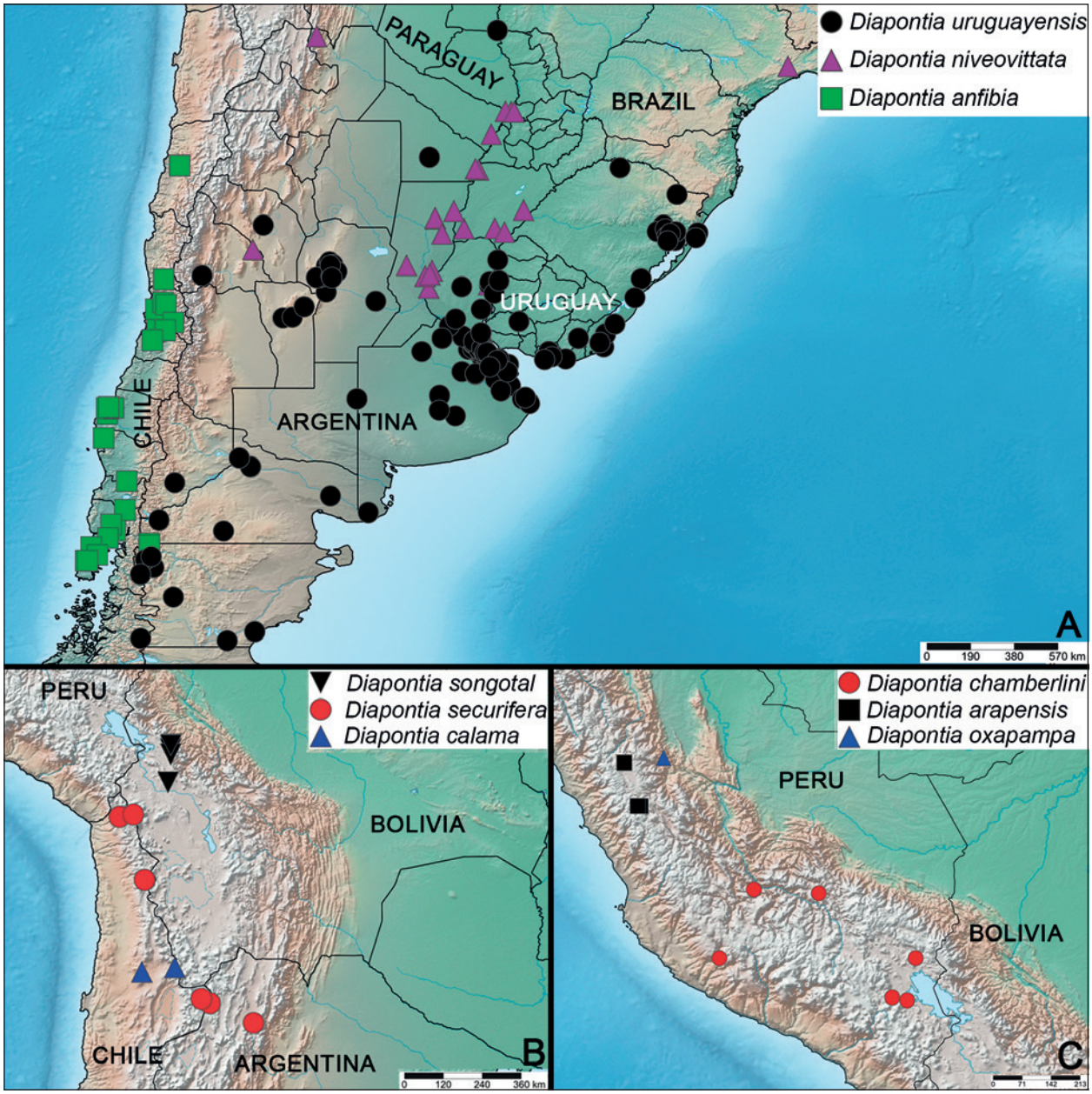

Fig. 20. Distribution records of *Diapontia* species. **A**: *Diapontia uruguayensis* Keyserling (black circle); *Diapontia niveovittata* Mello-Leitão (magenta triangle); *Diapontia anfibia* (Zapfe-Mann) **comb.n.** (green square). **B**: *Diapontia securifera* (Tullgren) **comb.n.** (red circle); *Diapontia calama* **sp.n.** (blue triangle); *Diapontia songotal* **sp.n.** (black invered triangle). **C**: *Diapontia arapensis* (Strand) **comb.n.** (black square); *Diapontia chamberlini* **sp.n.** (red circle); *Diapontia oxapampa* **sp.n.** (blue triangle).

loss of the funnel web on the different subfamilies of Lycosidae was suggested as a plausible scenario on the different subfamilies of Lycosidae by the reconstruction of ancestral states performed by Murphy et al. (2006). Species of *Aglaoctenus* and *Sosippus* spin a dense funnel web (Santos & Brescovit 2001; Brady 2007). In *Diapontia* we found that *D. uruguayensis*, *D. niveovittata* and *D. anfibia* spin a weak funnel web, while other representatives such as *D. chamberlini*, *D. songotal* and *D. securifera* were collected under stones without any trace of webs. Although there are little data on the natural history of *Hippasella*, the presence of adult males and females of *Hippasella alhue* in pitfall traps suggests a vagrant lifestyle (Piacentini 2011).

4.4. Biogeography

Although interpretations of biogeographical patterns for Lycosidae are usually difficult (Framenau 2010) the genera of Sosippinae show an interesting geographic structure. *Sosippus*, sister to all other sossippines, is restricted to Southern part of North America and Central America (Brady 2007), and the rest of the subfamily is exclusively South American Within these, *Aglaoctenus* (Santos & Brescovit 2001; Santos et al. 2003; Piacentini 2011) and *Diapontia* are known from Neotropical and Andean regions *sensu* Morrone (2014). The remaining genus, *Hippasella*, is restricted to the Andean region (Álvarez & Brescovit 2007; Piacentini 2011).

4.5. DNA barcode analysis

As was previously found in other wolf spider genera (Nadonly et al. 2016; Blagoev et al. 2013; Sim et al. 2014), the genetic barcode marker COI is not able to differentiate all species of *Diapontia*. We could successfully identify *D. securifera* and *D. anfibia* as definite BINs, but *D. niveovittata* and *D. uruguayensis* were not unambiguously separated. One BIN (ACY4930) is composed by two *D. niveovittata* from Entre Ríos and the other (ACY4931) by the remaining specimens of *D. niveovittata* and *D. uruguayensis* mixed together. Remarkably, one exemplar of BIN ACY4930 (MACN-Ar 30520) was collected at the same time and place as one exemplar of BIN ACY4931 (MACN-Ar 30519); both exemplars were re-examined and their identifications were confirmed *D. niveovittata* by morphological characters. The split in two BINs of *D. niveovittata* may be explained by the small size of the sample which has great impact on the power of resolution of the "barcode gap" (Meyer & Paulay 2005). Despite the small sample size, the presence of identical sequences in specimens of *D. niveovitatta* and *D. uruguayensis* indicate that this marker cannot be used to distinguish one from the other – a problem that is becoming more common as barcoding is applied to a growing list of closely related taxa. For example, this problem also occurs in two morphologically distinct wolf spider species that have identical COI sequences, *Pardosa lugubris* (Walckenaer, 1802) and *Pardosa alacris* (C.L. Koch, 1833), as reported by Nadolny et al. (2016) and the problem has also been realized for insects (Hebert et al. 2003; Burns et al. 2007; Raupach et al. 2010; Huemer et al. 2014; Klopfstein et al. 2016). The identical COI sequence may be the result of mitochondrial introgression caused by ongoing hybridization (Petit & Excoffier 2009; Klopfstein et al. 2016) or, alternatively, by maternally inherited symbionts such as *Wolbachia*, *Rickettsia* or *Spiroplasma*, which were reported in spiders (Lerette et al. 2006; Goodacre et al. 2006; Ceccarelli et al. 2016) and results in a considerable underestimation of species diversity using DNA barcoding (Whitworth et al. 2007). Improving methods to identify species of *Diapontia* using molecular markers will require the inclusion of more specimens and the use of nuclear markers such as ITS2 or rDNA that have been demonstrated to be good complements to COI (Raupach et al. 2010; Klopfstein et al. 2016).

5. Acknowledgements

We are indebted to all curators, collection managers and other museum staff who have contributed to this study by making their collections and specimens accessible: Norman Platnick (AMNH), Charles Griswold (CAS); Miguel Simó (FCE); Laura Leipisberger MCZ); Luis Pereira and Mónica Tassara (MLP); Mario Elgeta (MNHN); Diana Silva (MUSM); Jorge Artigas (MZUC-UCCC); Janet Beccaloni (NHM); Jonathan Coddington (USNM) and Andrés Taucare Ríos (Universidad de Chile). We thank Cristian Grismado, Eduardo Soto and Sara Ceccarelli for helpful comments on an earlier version of the manuscript. M.N. Carbajal would like to thank María Elena Galiano, who directed her undergraduate thesis on *Diapontia*, and Axel Bachmann who introduced her to this genus. L.N. Piacentini is especially thankful to Charles Griswold of the California Academy of Sciences and the Lakeside Fellowship that provided support to travel to San Francisco to participate in the Lycosoidea Summit, and to the American Museum of Natural History for a collection study grant. This study was primarily supported by grants from FONCyT PICT 2011-1007 and CONICET PIP 2012-943 to MJR and CNPq 301776/2004-0 grant to ADB. We thank the referees Petra Sierwald, Cor Vink and Volker Framenau for their comments on the manuscript. We are specially indebted to Dan Proud for his assistance with correcting the language and grammar and providing other helpful comments on the manuscript.

6. References

Álvares E.S.S., Brescovit A. 2007. A review of the wolf spider genus *Hippasella* (Araneae, Lycosidae, Sosippinae). – Journal of Arachnology **35**: 313–317.

Astrin J.J., Höfer H., Spelda J., Holstein J., Bayer S., Hendrich L. et al. 2016. Towards a DNA Barcode Reference Database for spiders and harvestmen of Germany. – PLoS ONE **11**(9): e0162624. doi:10.1371/journal.pone.0162624

Blagoev G.A., Dondale C.D. 2014. A new species of *Alopecosa* (Araneae: Lycosidae) from Canada: a morphological description supported by DNA barcoding of 19 congeners. – Zootaxa **3894**(1): 152–160.

Blagoev G.A., Nikolova N.I., Sobel C.N., Hebert P.D.N. & Adamowicz S.J. 2013. Spiders (Araneae) of Churchill, Manitoba: DNA barcodes and morphology reveal high species diversity and new Canadian records – BMC Ecology **13**: 44.

Brady A. 2007. *Sosippus* revisited: review of a web-bulding wolf spider genus from the Americas (Araneae, Lycosidae). – Journal of Arachnology **35**: 54–83.

Brescovit A., Álvares E.S.S. 2011. The wolf spider species from Peru and Bolivia described by Embrik Strand in 1908 (Araneae: Lycosidae: Lycosinae, Sosippinae, Allocosinae). – Zootaxa **3037**: 51–61.

Burns J.M., Janzen D.H., Hajibabaei M., Hallwachs W., Hebert P. 2007. PDN: DNA barcodes of closely related (but morphologically and ecologically distinct) species of skipper butterflies (Hesperiidae) can differ by only one to three nucleotides. – Journal of the Lepidopterists' Society **61**(Suppl 3): 138–153.

Capocasale R.M. 1982. Las especies del genero *Porrimosa* Roewer, 1959 (Araneae, Hippasinae). – Journal of Arachnology **10**: 145–156.

Casanueva M.E. 1980. Los licosidos de Chile. Estudio biológico y taxonómico por los métodos de sistematica alfa y taxonómica numérica (Araneae: Lycosidae). – Gayana (Zoologia) **42**: 1–76.

Casquet J., Thebaud C., Gillespie R.G. 2012. Chelex without boiling, a rapid and easy technique to obtain stable amplifiable DNA from small amounts of ethanol-stored spiders. – Molecular Ecology Resources **12**(1): 136–141.

Castresana J. 2000. Selection of conserved blocks from multiple alignments for their use in phylogenetic analysis. – Molecular Biology and Evolution **17**(4): 540–552.

Ceccarelli F.S., Haddad C.R., Ramírez M.J. 2016. Endosymbiotic *Rickettsiales* (Alphaproteobacteria) from the spider genus *Amaurobioides* (Araneae: Anyphaenidae). – Journal of Arachnology **44**(2): 251–253.

Chamberlin R.V. 1916. Results of the Yale Peruvian Expedition of 1911. The Arachnida – Bulletin of the Museum of Comparative Zoology at Harvard College **60**: 177–299.

Correa-Ramírez M.M., Jiménez M.L., García-De León F.J. 2010. Testing species boundaries in *Pardosa sierra* (Araneae: Lycosidae) using female morphology and COI mtDNA. – Journal of Arachnology **38**: 538–554.

Dolejs P., Buchar J., Kubcova L., Smrz J. 2006. Developmental changes in the spinning apparatus over the life cycle of wolf spiders (Araneae: Lycosidae). – Invertebrate Biology **133**(3): 281–297.

Dondale C.D. 1986. The subfamilies of wolf spiders (Araneae: Lycosidae). – Actas X Congreso Internacional de Aracnologia, Barcelona **12**(1): 327–332.

Dondale C.D., Redner J.H. 1990. The wolf spiders, nurseryweb spiders, and lynx spiders of Canada and Alaska. Araneae: Lycosidae, Pisauridae, and Oxiopidae. The Insects and Arachnids of Canada: 17. – Agriculture Canada, Canada.

Farley C., Shear W.A. 1973. Observations on the courtship behaviour of *Lycosa carolinensis*. – Bulletin of the British Arachnological Society **2**(8): 153–158.

Fuhn I.E., Niculescu-Burlacu F. 1971. Fam. Lycosidae. – Fauna Republicii Socialiste România (Arachnida) **5**(3): 1–253.

Framenau V.W. 2010. Revision of the new Australian wolf spider genus *Kangarosa* (Araneae: Lycosidae: Artoriinae). – Arthropod Systematics & Phylogeny **68**: 113–142.

Garrison N.L., Rodriguez J., Agnarsson I., Coddington J.A., Griswold C.E., Hamilton C.A., Hedin M., Kocot K.M., Ledford J.M., Bond J.E. 2016. Spider phylogenomics: untangling the spider tree of life. – PeerJ 4: e1719.

Griswold C.E. 1993. Investigations into the phylogeny of the lycosoid spiders and their kin (Arachnida: Araneae: Lycosoidea). – Smithsonian Contributions to Zoology **539**: 1–39.

Goodacre S.L., Martin O.Y., Thomas C.F.G., Hewitt G.M. 2006. *Wolbachia* and other endosymbiont infections in spiders. – Molecular Ecology **15**(2): 517–527.

Hall T.A. 1999. BioEdit: a user-friendly biological sequence alignment editor and analysis a program for Windows 95/98/NT. – Nucleic Acids Symposium Series **41**: 95–98.

Hebert P.D.N., Ratnasingham S., deWaard J.R. 2003. Barcoding animal life: cytochrome c oxidase subunit 1 divergences among closely related species. – Proceedings of the Royal Society **270**(B): S596–S599.

Hedin M.C., Maddison W.P. 2001. A combined molecular approach to phylogeny of the jumping spider subfamily Dendryphantinae (Aranae: Salticidae). – Molecular Phylogenetics and Evolution **18**: 386–403.

Hedin M.C. 1997. Molecular phylogenetics at the population/species interface in cave spiders of the southern Appalachians (Araneae: Nesticidae: Nesticus). – Molecular Biology and Evolution **14**: 309–324.

Huemer P., Mutanen M., Sefc K.M., Hebert P.D.N. 2014. Testing DNA barcode performance in 1000 species of european Lepidoptera: large geographic distances have small genetic impacts. – PloS ONE **9**(12): e115774.

Jocqué R., Alderweireldt M. 2005. Lycosidae: the grassland spiders. – Acta Zoologica Bulgarica **1**: 125–130.

Katoh K. Standley D.M. 2013. MAFFT multiple sequence alignment software version 7: improvements in performance and usability. – Molecular Biology and Evolution **30**: 772–780.

Klopfstein S., Kropf C., Baur H. 2016. *Wolbachia* endosymbionts distort DNA barcoding in the parasitoid wasp genus *Diplazon* (Hymenoptera: Ichneumonidae). – Zoological Journal of the Linnean Society **177**(3): 541–557.

Kocher T.D., Thomas W.K., Meyer A., Edwards S.V., Pääbo S., Villablanca F.X. 1989. Dynamics of mitochondrial DNA evolution in animals: amplification and sequencing of conserved primers. – Proceedings of the National Academy Sciences of the United States of America **86**: 6196–6200.

Lanfear R., Calcott B., Ho S.Y.W., Guindon S. 2012. PartitionFinder: combined selection of partitioning schemes and substitution models for phylogenetic analyses. – Molecular Biology and Evolution **29**(6): 1695–1701.

Langlands P., Framenau V.W. 2010. Systematic revision of *Hoggicosa* Roewer, 1960, the Australian 'bicolor' group of wolf spiders (Araneae: Lycosidae). – Zoological Journal of the Linnean Society **158**: 83–123.

Lehtinen P.T., Hippa H. 1979. Spiders of the Oriental-Australian region. I. Lycosidae: Venoniinae and Zoicinae. – Annales Zoologici Fennici **16**: 1–22.

Lerette S., Aisenberg A., Costa F., Sotelo-Silveira J.R., Bidegaray-Batista L. 2015. Detección de la bacteria endosimbionte *Wolbachia* en la araña lobo *Allocosa alticeps* y posibles efectos sobre la proporción. – Boletín de la Sociedad Zoológica del Uruguay (2ª época) **24**(2): 171–176.

Logunov D.V. 2010. On new central Asian genus and species of wolf spiders (Araneae: Lycosidae) exhibiting a pronounced sexual size dimorphism. – Proceedings of the Zoological Institute of the Russian Academy of Sciences **314**: 233–263.

Mello-Leitão C.F. de 1941. Las arañas de Córdoba, La Rioja, Catamarca, Tucumán, Salta y Jujuy colectadas por los Profesores Birabén. – Revista del Museo de La Plata (Nueva Serie, Zoología) **2**: 99–198.

Mello-Leitão C.F. de 1944. Arañas de la provincia de Buenos Aires. – Revista del Museo de La Plata (Nueva Serie, Zoología) **3**: 311–393.

Meyer C.P., Paulay G. 2005. DNA barcoding: error rates based on comprehensive sampling. – Plos Biology **3**: 1–10.

Miller M.A., Pfeiffer W., Schwartz T. 2010. Creating the CIPRES Science Gateway for inference of large phylogenetic trees. – Pp 1–8 in: Proceedings of the Gateway Computing Environments Workshop 14 Nov. 2010, New Orleans, LA.

Morrone J.J. 2014. Biogeographical regionalisation of the Neotropical region. – Zootaxa **3782**(1): 1–110.

Murphy N.P., Framenau V.W., Donellan S.C., Harvey M.S., Park Y.-C., Austin A.D. 2006. Phylogenetic reconstruction of the wolf spiders (Araneae: Lycosidae) using sequences from the 12S rRNA, 28S rRNA, and NADH1 genes: implications for classification, biogeography, and the evolution of web building behavior. – Molecular Phylogenetics and Evolution **38**: 583–602.

Nadolny A.A., Omelko M.M., Marusik Y.M., Blagoev G. 2016. A new species of spider belonging to the *Pardosa lugubris*-group (Araneae: Lycosidae) from Far East Asia. – Zootaxa **4072**(2): 263–281.

Petrunkevitch A. 1911. A synonymic index-catalogue of spiders of North, Central and South America with all adjacent islands, Greenland, Bermuda, West Indies, Terra del Fuego, Galapagos, etc. – Bulletin of the American Museum of Natural History **29**: 1–791.

Piacentini L.N. 2011. Three new species and new records in the wolf spider subfamily Sosippinae from Argentina (Araneae: Lycosidae). – Zootaxa **3018**: 27–49.

Piacentini L.N. 2014. A taxonomic review of the wolf spider genus *Agalenocosa* Mello-Leitão (Araneae, Lycosidae). – Zootaxa **3790**(1): 1–35.

Piacentini L.N., Grismado C.J. 2009. *Lobizon* and *Navira*, two new genera of wolf spiders from Argentina (Araneae: Lycosidae). – Zootaxa **2195**: 1–33.

Petit R.J., Excoffier L. 2009. Gene flow and species delimitation. – Trends in Ecology & Evolution **24**(7): 386–393.

Polotow D., Carmichael A., Griswold C. 2015. Total evidence analysis of the phylogenetic relationships of Lycosoidea spiders (Araneae, Entelegynae). – Invertebrate Systematics **29**(2): 124–163.

Rambaut A., Suchard M., Xie W., Drummond A. 2014. Tracer v. 1.6. – Institute of Evolutionary Biology, University of Edinburgh.

Ramírez M.J. 2003. The spider subfamily Amaurobioidinae (Araneae, Anyphaenidae): a phylogenetic revision at the generic level. – Bulletin of the American Museum of Natural History **277**: 1–262.

Ramírez M.J. 2014. The morphology and phylogeny of dionychan spiders (Araneae: Araneomorphae). – Bulletin of the American Museum of Natural History **390**(1): 1–374.

Ratnasingham S., Hebert P.D.N. 2007. BOLD: The Barcode of Life Data System (www.barcodinglife.org). – Molecular Ecology Notes **7**: 355–364.

Raupach M.J., Astrin J.J., Hannig K., Peters M.K., Stoeckle M.Y., Wägele J. 2010. Molecular species identification of central european ground beetles (Coleoptera: Carabidae) using nuclear rDNA expansion segments and DNA Barcodes. – Frontiers in Zoology **7**(1): 26.

Roberts J.A., Uetz G.W. 2005. Information content of female chemical signals in the wolf spider, *Schizocosa ocreata*: male discrimination of reproductive state and receptivity. – Animal Behaviour **70**: 217–223.

Roewer C.F. 1955. Katalog der Araneae von 1758 bis 1940, bzw. 1954. 2. Band, Abteilung A (Lycosaeformia, Dionycha [excl. Salticiformia]). – Institut Royal des Sciences Naturelles de Belgique, Bruxelles. 923 pp.

Roewer C.F. 1960. Araneae Lycosaeformia II (Lycosidae) (Fortsetzung und Schluss). – Exploration du Parc National de l'Upemba, Mission G. F. de Witte **55**: 519–1040.

Ronquist F., Klopfstein S., Vilhelmsen L., Schulmeister S., Murray D.L., Rasnitsyn A.P. 2012. A total-evidence approach to dating with fossils, applied to the early radiation of the Hymenoptera. – Systematic Biology **61**: 973–999.

Rosenberg M.S., Kumar S. 2003. Heterogeneity of nucleotide frequencies among evolutionary lineages and phylogenetic inference. – Molecular Biology and Evolution **20**: 610–621.

Rovner J.S. 1974. Copulation in the lycosid spider *Schizocosa saltatrix* (Hentz): an analysis of palpal insertion patterns. – Animal Behaviour **22**: 94–99.

Rypstra A.L., Wieg C., Walker S.E., Persons S.H. 2003. Mutual mate assessment in wolf spiders: Differences in the cues used by males and females. – Ethology **109**: 315–325.

Santos A.D., Brescovit A.D. 2001. A revision of the South American spider genus *Aglaoctenus* Tullgren, 1905 (Araneae, Lycosidae, Sosippinae). – Andrias **15**: 75–90.

Santos A.D., Álvares E.S.S., Brescovit A.D. 2003. On the third valid species of the genus *Aglaoctenus* Tullgren (Araneae, Lycosidae). – Revista Ibérica de Aracnología **8**: 89–92.

Schmidt H.A., Strimmer K., Vingron M., Von Haeseler A. 2002. Tree-Puzzle: maximum likelihood phylogenetic analysis using quartets and parallel computing. – Bioinformatics **18**: 502–504.

Sierwald P. 2000. Description of the male of *Sosippus placidus*, with notes on the subfamily Sosippinae (Araneae, Lycosidae). – Journal of Arachnology **28**: 133–140.

Sim K.A., Buddle C.M., Wheeler T.A. 2014. Species boundaries of *Pardosa concinna* and *P. lapponica* (Araneae: Lycosidae) in the northern Nearctic: morphology and DNA barcodes. – Zootaxa **3884**(2): 169–178.

Simon E. 1898. Histoire Naturelle des Araignées. – Roret, Paris, pp. 193–380.

Stamatakis A. 2014. RAxML Version 8: A tool for phylogenetic analysis and post-analysis of large phylogenies. – Bioinformatics **30**: 1312–1313.

Strand E. 1908. Exotisch araneologisches. – I. Amerikanische hauptsächlich in Peru, Bolivien und Josemitetal in Californien gesammelte Spinnen. – II. Spinnen aus Kamerun. – III. Übersicht der bekannten Hysterocrates-Arten. – IV. Zur Kenntnis der Araneae rufipalpis (Luc). – Jahrbücher des Nassauischen Vereins für Naturkunde **61**: 223–295.

Townley M.A., Tillinghast E.K. 2003. On the use of ampullate gland silks by wolf spiders (Araneae, Lycosidae) for attaching the egg sac to the spinnerets and a proposal for defining nubbins and tartipores. – Journal of Arachnology **31**: 209–245.

Tullgren A. 1905. Aranedia from the Swedish expedition through the Gran Chaco and the Cordilleras. – Arkiv för Zoologi **2**(19): 1–81.

Wheeler W., Coddington J., Crowley L., Dimitrov D., Goloboff P., Griswold C., Hormiga G., Prendini L., Ramirez M., Sierwald P., Almeida-Silva L., Alvarez-Padilla F., Arnedo M., Benavides Silva L., Benjamin S., Bond J., Grismado C., Hasan E., Hedin M., Izquierdo M., Labarque F., Ledford J., Lopardo L., Maddison W., Miller J., Piacentini L., Platnick N., Polotow D., Silva-Davila D., Scharff N., Szuts T., Ubick D., Vink C., Wood H., Zhang J. 2017. The spider tree of life: phylogeny of Araneae based on target-gene analyses from an extensive taxon sampling. – Cladistics **33**(6): 574–616.

Whitworth T.L., Dawson R.D., Magalon H., Baudry E. 2007. DNA Barcoding cannot reliably identify species of the blowfly genus *Protocalliphora* (Diptera: Calliphoridae). – Proceedings of the Royal Society of London B: Biological Sciences **274**(1619): 1731–1739.

Zapfe-Mann H. 1979. *Pardosa anfibia*, nueva especie (Lycosidae, Araneae). – Noticiario mensual del Museo Nacional de Historia Natural, Santiago **272**: 3–7.

Electronic Supplement Files

at http://www.senckenberg.de/arthropod-systematics

File 1: piacentini&al-diapontiaspiders-asp2017-electronicsupplement-1.doc — Material examined: non-type specimens.

File 2: piacentini&al-diapontiaspiders-asp2017-electronicsupplement-2.doc — Data on barcode gap. — **Table S2.1** Summary of the genetic distances of *Diapontia* species, numbers on the middle diagonal line correspond to the intraspecific variations. — **Table S2.2** Genetic divergence values for each species, the mean (MID) and maximum intra-specific values are compared to the nearest neighbor. — **Fig. S2.3** A plot of the maximum intraspecific distance compared with distance to nearest neighbor of all species of the genus *Diapontia* used in this study. — **Table S2.4** List of specimens of *Diapontia* used on the BARCODE DNA analysis. — **Fig. S2.5** Tree obtained under maximum likelihood analysis, values on the nodes indicate the boostrap values.

Zoobank registrations

at http://zoobank.org

Present article: http://zoobank.org/urn:urn:lsid:zoobank.org:pub:1B737C59-4120-4CF6-A5E1-9438186F115D

***Diapontia calama* Piacentini, Scioscia, Carbajal, Ott, Brescovit & Ramírez, 2017:** http://zoobank.org/urn:lsid:zoobank.org:act:3BC04023-FA55-4CFA-9B98-54A08870F86B

***Diapontia songotal* Piacentini, Scioscia, Carbajal, Ott, Brescovit & Ramírez, 2017:** http://zoobank.org/urn:lsid:zoobank.org:act:C90807E9-8270-42CA-AF90-296C95305BE8

***Diapontia chamberlini* Piacentini, Scioscia, Carbajal, Ott, Brescovit & Ramírez, 2017:** http://zoobank.org/urn:lsid:zoobank.org:act:2FAC327A-FB58-4720-B123-B1F7E6863EDF

***Diapontia oxapampa* Piacentini, Scioscia, Carbajal, Ott, Brescovit & Ramírez, 2017:** http://zoobank.org/ urn:lsid:zoobank.org:act:590C58DD-CAF5-4BFD-99FC-CF83A76FA5C4